Since January 2020 Elsevier has created a COVID-19 resource centre with free information in English and Mandarin on the novel coronavirus COVID-19. The COVID-19 resource centre is hosted on Elsevier Connect, the company's public news and information website.

Talanta 221 (2021) 121615

Contents lists available at ScienceDirect

Talanta

journal homepage: www.elsevier.com/locate/talanta

Photonic crystal based biosensors: Emerging inverse opals for biomarker detection

Farzaneh Fathi [a,*], Mohammad-Reza Rashidi [b], Parvin Samadi Pakchin [c], Sohrab Ahmadi-Kandjani [d], Arash Nikniazi [d,e]

[a] Pharmaceutical Sciences Research Center, Ardabil University of Medical Sciences, Ardabil, Iran
[b] Faculty of Pharmacy, Tabriz University of Medical Sciences, Tabriz, Iran
[c] Research Center for Pharmaceutical Nanotechnology, Biomedicine Institute, Tabriz University of Medical Sciences, Tabriz, Iran
[d] Photonics Group, Research Institute for Applied Physics and Astronomy, University of Tabriz, Tabriz, Iran
[e] Department of Physics, Engineering Physics & Astronomy, Queen's University, Kingston, Ontario, Canada

ARTICLE INFO

Keywords:
Photonic crystal
Inverse opal
Biomarker detection

ABSTRACT

Photonic crystal (PC)-based inverse opal (IO) arrays are one of the substrates for label-free sensing mechanism. IO-based materials with their advanced and ordered three-dimensional microporous structures have recently found attractive optical sensor and biological applications in the detection of biomolecules like proteins, DNA, viruses, etc. The unique optical and structural properties of IO materials can simplify the improvements in non-destructive optical study capabilities for point of care testing (POCT) used within a wide variety of biosensor research. In this review, which is an interdisciplinary investigation among nanotechnology, biology, chemistry and medical sciences, the recent fabrication methodologies and the main challenges regarding the application of (inverse opals) IOs in terms of their bio-sensing capability are summarized.

1. Introduction

Todays the employing of biosensors for detecting a wide range of diseases in clinical experiments has been revealed for everyone. Biosensors mediated optical measurements have usually proven to be reliable, faster, compact, and user-friendly than those applying electrochemical and conventional optical bio-sensing systems [1,2]. Sensitive bio-sensing technologies such as surface plasmon resonance (SPR), electrochemical biosensors and recently inverse opal photonic crystals (IOPCs) biosensors, have been employed as diagnostic devices for the detection of biomarkers [3–8]. Photonic crystals (PCs) are dielectric and nanostructured materials with optical sensing properties and wide range applications in the field of optoelectronics and photonics [9–11]. Presently, PCs biosensors have been used for the selectively and sensitively detection of various biological analytes, such as DNA, cells, pathogens, proteins, antibodies (Ab) allows enhancing sensing performance in terms of limit-of-detection (LOD) [12,13].

In addition, the importance and relationship between the physico-chemical properties and the structure of the materials such as size, shape, and type are more than ever known to the researchers. The special shape and size of nanomaterials was included nanospheres, nanofibers, nanorods, nanoporous and nanocrystals, which can enhance the performance of the nano-structural biosensors [14]. PCs, which have unique physical and optical properties, for the first time was introduced by Yablonovitch in 1987 [15]. They reported the high-dimensional periodic optical structures of PCs by the engineering photonic density of states to control the spontaneous emission of materials embedded in the PCs [15]. The scientific history of IOs demonstrating was shown in Scheme 1.

PCs like liquid crystals, IOs and PCs fibers are now being widely implemented in bio-sensing works [18–20]. PCs that affect the motion of photons are novel nanostructures of optical media with spatial modulation of the refractive index periodically [21]. In natural or artificial PCs structures, the formation of the photonic bandgap (PBG) in the crystals is due to the periodic arrays of the refractive index [22]. Based on PCs geometry, the periodicity of PCs can be repeated in one, two or three directions which indicate the different dielectric constants in PC structures [23,24].

Until now, various reviews in the field of PCs bioassays and their application in bio-systems with focusing on the physical and optic

* Corresponding author.
E-mail addresses: f.fathi@arums.ac.ir, fathifa@tbzmed.ac.ir (F. Fathi).

https://doi.org/10.1016/j.talanta.2020.121615
Received 24 April 2020; Received in revised form 2 August 2020; Accepted 28 August 2020
Available online 2 September 2020

behavior of PCs have been published [24–26]. However, it seems that IOPCs based biosensors need to be articulated much more comprehensively with some highlights and insights on the fabrication and detection of special biomarkers using IOs in clinical application [27,28]. In this review, we provide a comprehensive overview and insights on the IOs bio-sensing mechanisms for the detection of biological components like viruses, protein, DNA, etc.

2. An overview to IO PC structures and fabrications

To better understanding IO structures, it is important to first know about the concept of PC and opaline arrays. PCs defined as the highly ordered structures which have a variation in dielectric constant and the scale of visible light wavelengths (400–800 nm) periodically [29]. The opaline films which are PCs materials usually were formed by polystyrene (PS), polymethyl methacrylate (PMMA) and silica (SiO_2) nano or microspheres on the glass substrate [30]. The formed films using microspheres with a diameter between 100 and 500 nm are highly porous and have specific optical properties [31].

The periodical arrays of the refractive index and the Bragg reflections on the lattice structure of PCs led to forbid light propagation within the interference of crystal and result in the formation of a PBG or stop band [32]. The energy shift between the valence band maximum and the bottom of the conduction band is called the electronic gap or band gap [33]. Similar to the electron flow in semiconductor structures, in PCs structures, photons move and the prohibiting of photons propagation in all directions and every state of polarization makes a complete or full PBG which is a unique characteristic of PCs [33]. Also, a pseudogap in PCs implies an incomplete PBG in which, forbid photons and a range of wavelengths propagation in some directions, not all directions [34]. A full PBG refers to organized structures with periodic lattice topology and morphology of various materials such as polymer microspheres used in IOs. The presence of the PBG and the ability of PCs to change the spectra position at specific frequencies introduced them as the most interesting and useful materials for sensing applications. Many methods have been developed for the fabrication of highly ordered three-dimensional (3D) PCs [11,35,36]. The PBG corresponds to the reflection of light by a periodic arrays and there is no absorbing of light in the process. PCs structure includes three groups based on their geometry: one-dimensional PC (1DPC), two-dimensional PC (2DPC) and three-dimensional PC (3DPC). PCs sensors using the PBG effect exert the sensitivity of PCs dispersion bands to develop their refractive index with gases or fluids [37]. Optical sensing can be detected in the simplest form by the monitoring of the PC reflectivity shift or transmission spectra [38]. In a 1DPC, a refractive index distributes along one direction of a periodic array of PCs nanostructure. Moreover, it has newly been proven that this dimensionally porous material showed perfectly optical sensing properties [39].

PCs include direct opal and IOs. The direct opals formed by self-assembly of colloid microspheres used as a template for IO with a cubic packing structure similar to natural opal [22]. Fig. 1 represents the overall imaging of natural opals and artificial PCs including opal and IO and also the schematic representation of 1D, 2D, and 3D PCs along with their SEM images was presented.

Due to having 3D ordered nanostructure and optical features in IO based PCs, they can use in biosensor applications. Natural PCs are responsible for colorful displays in some opaline stone, butterfly wing, and peacock feathers and also some plants [42–46]. IOs structures usually formed by 3D ordered microsphere materials using the infiltration of a synthetic opal with a filling material precursor-like TiO_2, ZnO, SiO_2 and polymers, and finally the elimination of the opal template [22]. The use of a high refractive index material in the preparation of IOs leads to achieving a comprehensive PBG in spectral analysis. In preparation of IOPCs via the colloidal crystal template technique, generally, PS, PMMA or SiO_2 microspheres are orderly arranged into opal PC templates [47]. The PCs were prepared through gravity sedimentation or centrifugal sedimentation, self-assembly, evaporation, dip coating or electrophoresis methods [48–50]. Then various target materials or precursor is filled in the prepared opal PCs template using deposition or hydrolysis. Lastly, after removing colloidal crystal templates by calcination or etching, the IOs PCs were fabricated. The periodic structure of the IOs guaranteed that photonic gaps or pseudogaps in the transparency section of the filled target material. IOs based on main filling target materials including zinc oxide (ZnO), titanium dioxide (TiO2), SiO2, polymer hydrogel and carbon IOs.

The deposition of filling materials can be done by several procedures, such as sol-gel chemistry, electrodeposition, spray pyrolysis, e-beam evaporating, the atomic layer and chemical vapor depositions, sputtering and thermal evaporation [51–57].

For example, ZnO IOs films with several hundred IO domains were fabricated using a simple sol-gel technique [58]. This method comprising infiltration of PS colloidal crystal templates with a saturated water-alcohol solution of zinc nitrate, drying, heating, and annealing at 300 °C for 12 h. Colloidal crystal films were fabricated by a vertical deposition method, performed in aqueous suspension of 450 nm PS microspheres, on glass substrates [58]. Also, ZnO PC structures were fabricated by the ZnO sol-gel solution and a spin coating method [59]. In this method, inverted ZnO PC structures were developed using self-assembling of 200 nm PS suspension onto the glass slides by horizontal assembly technique in spin coating process. Then the sol-gel ZnO solution containing zinc acetate, ethanolamine, and alcohol was deposited on the substrates at 60 °C within 90 min stirring. Finally, inverted ZnO photonic structures along with ZnO nanoparticles were synthesized by removing the PS under a thermal treatment at 400 °C, as shown in Fig. 2a The obtained inverted ZnO PC structures have a hexagonal compact arrangement shapes. These structures have the PBG in

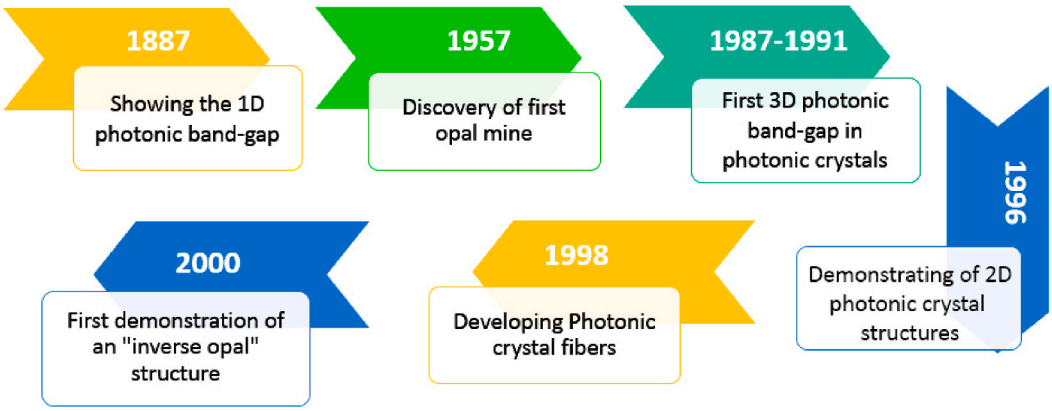

Scheme 1. Schematic of significant developments in the history of IOs [9,15,16]. As shown, the first development of IOs was in 2000 [17] IOs: Inverse opals.

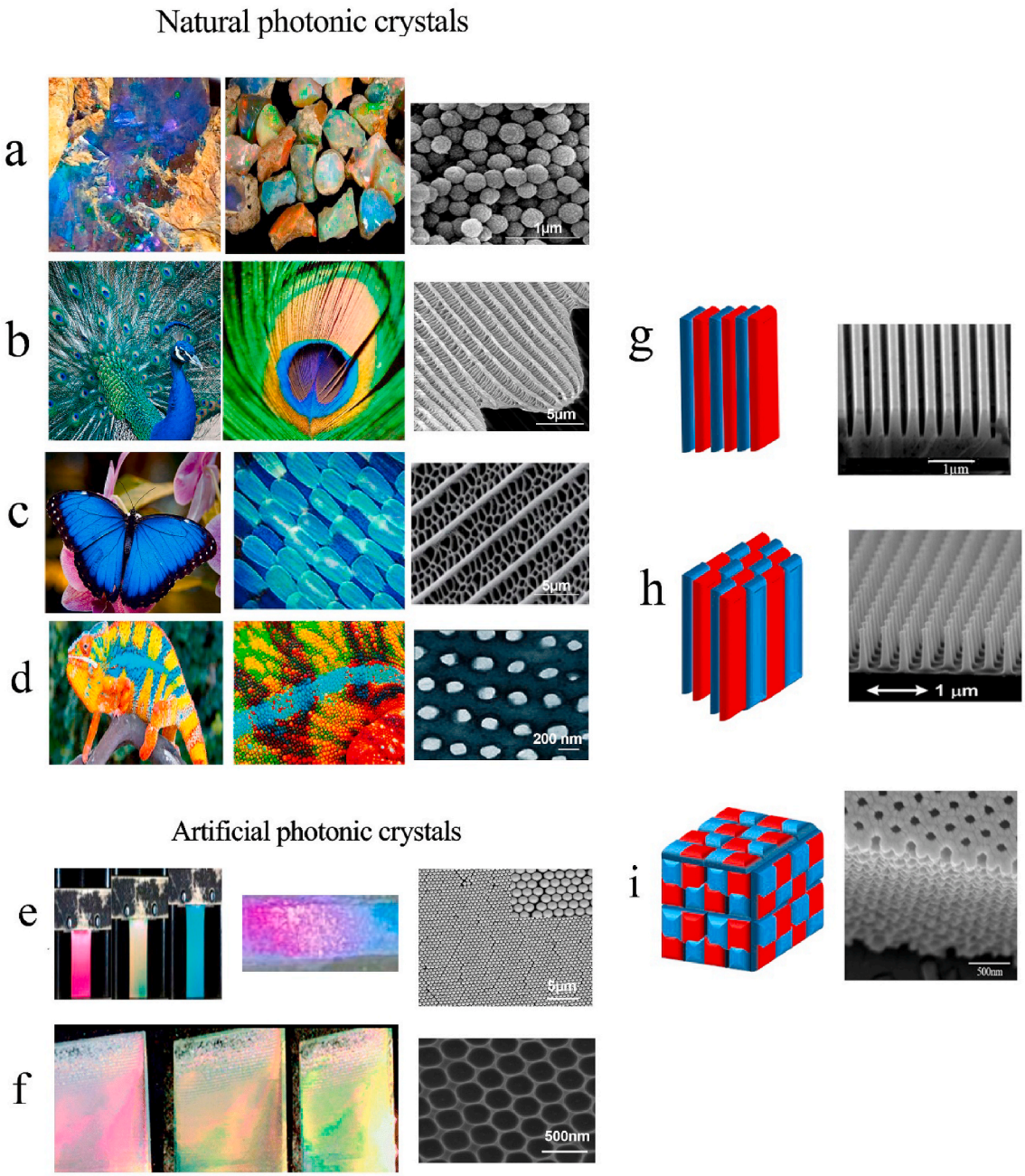

Fig. 1. Natural PCs: a) mine stone b) peacock feathers c) butterfly wing d) chameleon skin and artificial: e) PCs opal films f) IOs. Schematic representation of PCs structures g) 1D h) 2D i) 3D (the red and blue colors representing periodicity in 1D, 2D, and 3D PCs) with related SEM images. Copyright 2019, Royal Society of Chemistry. Reproduced from Ref. [40]. Copyright 2008, International Society for Optics and Photonics. Reproduced from Ref. [41]. (PCs: photonic crystals, IOs: inverse opals, 1D: One-dimensional, 2D: Two-dimensional, 3D: Three-dimensional, SEM: Scanning electron microscopy). (For interpretation of the references to color in this figure legend, the reader is referred to the Web version of this article.)

the ultraviolet (UV) ranges and display an improved photoluminescence peaks [59].

PCs based TiO_2 IOs with possessing of the TiO_2 material advantages including non-toxicity, stability, high refractive index, and the optical features of PCs like having the pore structures, PBG, slow light, and refraction effects, and also photonic localization have an extensive application in the photocatalysis, biosensor, solar cell, and PC fiber [60–62]. The investigation of fabrication methods and the application of TiO_2 IOs have been a research hotspot in the field of photonic materials. TiO_2 IOs were usually prepared by the colloidal crystal template system. During the fabrication, PS nanospheres or microspheres or SiO_2 via orderly sedimentation were arranged as a template for filling target materials into opal PCs. Several conventional approaches have been employed to the fabrication of the TiO_2 microcavities structures including sol-gel method and etching techniques like an electrochemical deposition [63] (Fig. 2b).

Silica based IOs structures for the first time has developed by Jiang et al., in 1999. They have reported a reliable method for the production of colloidal SiO_2-based PCs which is regularly called “controlled-evaporation” or “vertical deposition” method [64]. Using this particular approach, SiO_2 atoms were deposited vertically on the template by evaporating the suspension of the solvent [65]. 3D SiO_2 IOs structures were fabricated from an aqueous colloidal suspension containing the PMMA microspheres and tetraethylorthosilicate (TEOS) sol solution via

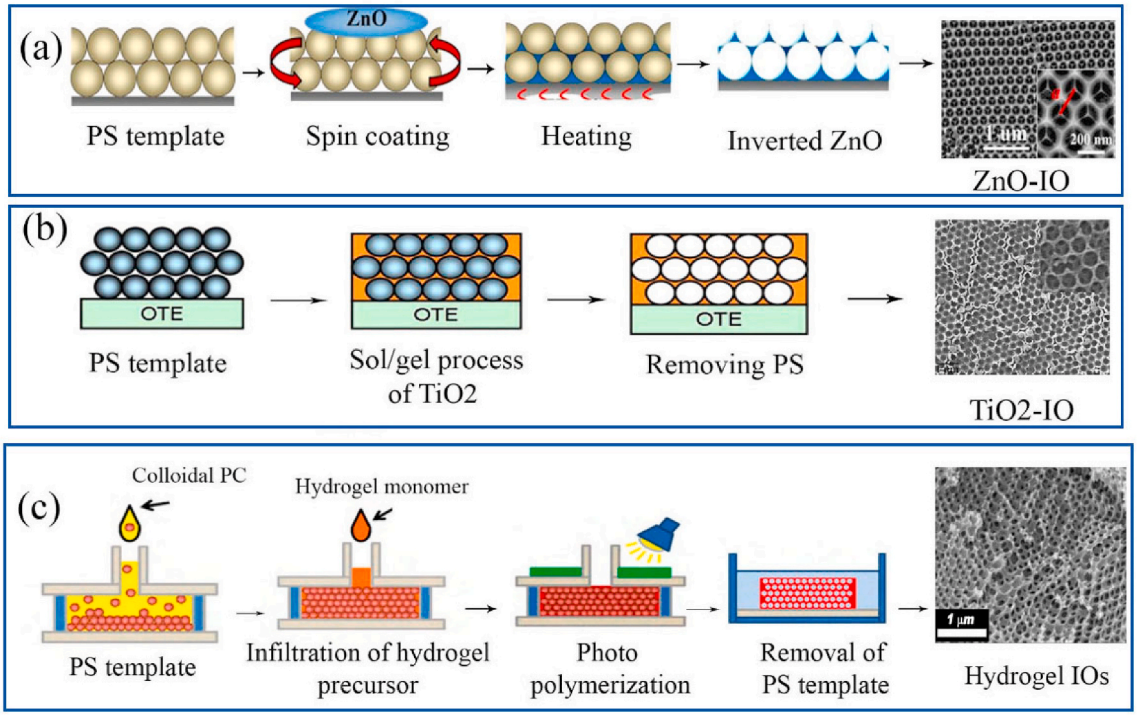

Fig. 2. Various methods for IOs synthesis. Fabrication of a) ZnO IOs using spin coating [59] b) TiO_2 IOs using sol/gel c) IOH photopolymerization. Copyright 2009, Elsevier. Reproduced from Ref. [80]. Copyright 2010, Elsevier. Reproduced from Refs. [78], IOs: Inverse opals, ZnO: Zinc oxide, TiO_2: Titanium dioxide.

controlled evaporation self-assembly methods [66]. The self-assembly methods as a bottom-up colloidal synthesis approaches compared with top-down methods have the simple processing steps and the prospect of the economically practical production 3D PC materials from simple colloidal particles [67]. The preparation of high-quality IOs on the inner or outer surface of large space with good interconnectivity and shapes is difficult through usual methods [68,69].

Carbon invers opals (CIOs) with porous 3D ordered structures, excellently diffracting light and absorbing hydrogen, provide examples of PBG PC materials. CIOs as a novel-structure carbon material has wide applications in optical and electrical fields, such as optics activator, storage battery, superconductivity nanostructures and other fields, such as absorption, separation, catalysis, and so on [70–72]. Many researchers have prepared CIOs with different monomers as precursors. For example, Tabata et al. reported the preparation of macroporous CIOs using various diameters of SiO_2 spheres as a template [73]. After filtering the SiO_2 spheres suspension on a nitrocellulose membrane, the membrane was condensed at a temperature above 1000 °C to improve the strength of the SiO_2 template. Then a mixture of furfuryl alcohol and oxalic acid was transferred into the space between the SiO_2 IOs for polymerization of alcohol and formation of resin in the interstice of the SiO_2 templates. Finally, after the carbonization of resin in argon atmosphere and etching of the SiO_2 particles, CIOs were prepared. The obtained CIOs were hard carbons, generally containing amorphous incompletely graphitized structures, and have good electronic conductivity [73].

For preparation of invers opal hydrogel (IOH), recently, the interstitial space of voids in a self-assembled PCs template was filled by hydrogel monomers (polyacrylamide, poly(dimethylaminoethyl methacrylate), acrylic acid) which can display distinct diffraction response with the changing of external stimulus, such as, pH, thermal, ionic strength, humidity or specific chemical functions [74–77]. The elastic properties of flexible hydrogel polymers make them suitable materials for monitoring the voids volume and refractive index changes in the IOs structures. For example, humidity IOH sensors were developed by a polyacrylamide hydrogel structure which able to respond to any variations in surroundings humidity detected by shifting its optical reflection peak in the visible region [77]. Developed IOH biosensors compared with usual IOs have a faster reaction speed and firmer mechanical strength which is related to mesoporous and flexible structure in IOH. IOH sensor for fast and visual detection of pH and specific chemical solutions was prepared by photo and radical polymerization of hydroxyethyl methacrylate monomers respectively (Fig. 2c) [78,79].

3. Detection mechanism in IO biosensors

IOs structures with periodic arrays due to having high and low dielectric zones are able to form photonic Bragg diffraction planes. This optical property produced by the photonic band led to use them in biosensing systems. The detection mechanism in IOs structures is related to the change in refractive index in the pores and voids of IOs films by binding of biomarkers on pore surfaces or flowing the liquids in IOs pores. This changes led to the blue/red shift in PBG position in reflected wavelength spectra and also color changes in IOs films [28].

The porous structure of the IOs makes a big surface area for the detection of small molecules. The highly-ordered IO is anticipated to have good optical properties. The various pores size in IOs led to have different reflection or transmittance spectra in optical investigations. In Fig. 3a, the reflection spectra of the TiO2 IOs with different pore size (188, 229, 279 and 320 nm) in water was shown [81]. Their stop band wavelengths was observed at 475 nm, 524 nm, 604 nm and 757 nm which had red shift with increasing the pore size. Also, the high reflection peak intensity reveals the deep stop bands of the IOs films. In Fig. 3b, the detection mechanism for protein based biomarkers like IgG was shown. As seen in this figure, the reflectance spectra of microcavity IOs film after the attachment of IgG, and also after the binding of goat anti-human IgG on the pore surfaces produced red shifts in peak [82]. The reason of observed red shifts come from two issues. First, the protein solution will change the mean refractive index of the IOs structure surface. The second factor is related to the bind of protein on the IOs pore surfaces [83]. Also, the shifts made by anti-IgG interaction with the immobilized IgG increased proportionally with increasing the anti-IgG

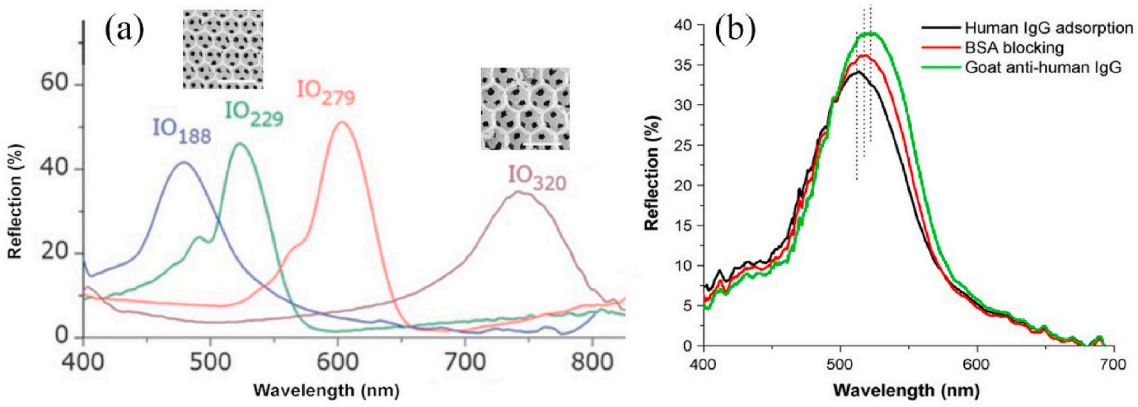

Fig. 3. a) The reflection spectra of the TiO_2 IOs with different pore size; Inset: SEM images of IO structures with 229 nm and 320 nm pore size (scale bar: 500 nm b) In situ reflectance spectra showing the immobilization of IgG, the blocking of BSA, and the binding of goat anti-human IgG on the pore surfaces.) Copyright 2012, Royal Society of Chemistry. Reproduced from Refs. [81] Copyright 2008, Elsevier. Reproduced from Ref. [82].

concentrations.

4. Sensing of biomarkers based on IOs

Optical based biosensors have demonstrated additional valuable qualities compared to other sensing methods that rely on electrochemical, thermal or mechanical properties [84].

Bio-sensing based on micro and nano-structured IO PCs which are very sensitive to refractive index changes is promising techniques in the formation of PBG and optoelectronics technology as well as in the field of optical biosensors [85]. Diagnosis and detection of biomaterials in IO optical biosensors are based on the monitoring of PC voids reflectivity or transmission spectra which infiltrated or modified by numerous biomolecules and fluids. More advanced IO PCs biosensors for sensitive detection of various biomolecules such as gases, proteins, glucose have been recently developed and implemented to expand the limit of detection [86,87]. 3D opal structures based PC are more attractive than 1D 2D PCs for the optical sensing applications. SiO_2 or PS microspheres are commercially available and the multiple regions of photonic gaps in fabricated opal structures exist [10,88]. The 3D structures have extensive capacities to increase the light-matter interactions and subsequently make stronger optical data. These diverse directions in the 3D IOs can make a favorable potency of integrating simultaneous optical detection at several wavelengths along with several directions [89]. In IO biosensors, photonic gaps are twice-higher sensitive than direct opals to the changes of environment refractive index. IO based biosensors not only have high sensitivity but also provide the application of them in thermally and chemically harsh environments. A biosensor is an analytical device that consists of a biological element and a physio-chemical transducer [3]. All biosensors have three main parts including, the biological recognition elements (like various target biomolecules, nucleic acids, enzymes, Abs, etc), a transducer which can transform the bio-response unit into a quantifiable signal (such as electrochemical, optical and piezoelectric transducers in electrochemical, SPR and QCM based biosensors), and finally a response processing system that exchanges the signal into a readable output [90,91].

4.1. Glucose detection

The sensing of blood glucose in clinical practice especially in the management of diabetes has been a valuable tool. The standard clinical amount for blood glucose is between 3.5 and 6.1 mM, but abnormal glucose levels can reach as high as 18 mM [92]. Therefore, to maintain the usual blood glucose ranges, the development of point-of-care devices for the detection of glucose has been recommended. The glucose biosensor based on the oxidation of glucose via molecular oxygen was designed [93]. Glucose oxidase (GOx) is a low cost catalyze enzyme that caused the oxidation of glucose. Flavin adenine dinucleotide (FAD) in GOx works as the first electron acceptor and is reduced to $FADH_2$. The produced hydrogen peroxide is oxidized by using a positive potential to the platinum anodic as a working electrode. The number of electron currents was monitored on the anode electrode which finally the obtained electrochemical transfer determine the glucose levels present in the blood [94].

Numerous types of biosensors like SPR, quartz crystal microbalance (QCM), electrochemical and optical biosensors have been developed for monitoring of glucose ranges in blood by GOx [95–98]. In SPR optic based gluco-sensor, GO was immobilized on to the gold sensor surface and after injection of gluconic acid and hydrogen peroxide glucose detection was provided by increase the refractive index and change the plasmonic condition of SPR curves [99]. The sensitivity of glucose biosensors are limited by the amount of the immobilized GOx enzyme on the sensor surface [100]. So the increase of loaded enzyme on the sensor surface led to improve in its sensitivity. For this purpose, with immobilizing GOx onto the selenium nanoparticle-mesoporous silica structures, an electrochemical enzymatic biosensor was developed for sensitive detection of glucose [95].

In IOs based biosensors, using nano structures of ZnO IOs, Xueqiu et al. reported the enzymatic glucose biosensors that have wide liner ranges due to decreased glucose diffusivity via the unique geometry of IOs [101]. Although different types of ZnO nanostructures such as nanoparticles, nanonails, nanocombs, nanorods, etc have been used for enzymatic glucose detection, but they have small liner ranges from 0.01 to 13.15 mM. In the developed ZnO IO biosensor, the linear detection range for glucose (between 0.01 and 18 mM) is 2.5 times larger than that of other described ZnO sensors [101]. These mechanical robust structures of IOs offer a proper microenvironment for enzyme attachment with durable stability. Also, the surface region of the ZnO IO is 25 times greater than that of in flat gold electrode (Fig. 4a). ZnO IO biosensor was synthesized by the sol-gel method for photoelectrochemical glucose detection using the acrylate as a template with a sensitivity of 52.4 $\mu A/mMcm^2$ [6]. In this study the enzymatic photoelectrochemical glucose biosensor was fabricated using modified ZnO IO structures with Nafion and GOx on the fluorine-doped tin oxide (FTO) electrode surface as seen in Fig. 4b.

A dual response reporter (optical and electrochemical signals) glucose biosensor based on IO conducting hydrogel films was described by Jin et al. [102]. Fig. 4c illustrates the crystalline IO arrays were fabricated by SiO_2 suspension as a template for polyacrylamide (PAA) hydrogel film. The thiophene conductive polymer was polymerized chemically within the IO hydrogel film. After covalent attachment of GOX on the IO backbone, the microenvironment of the hydrogel was

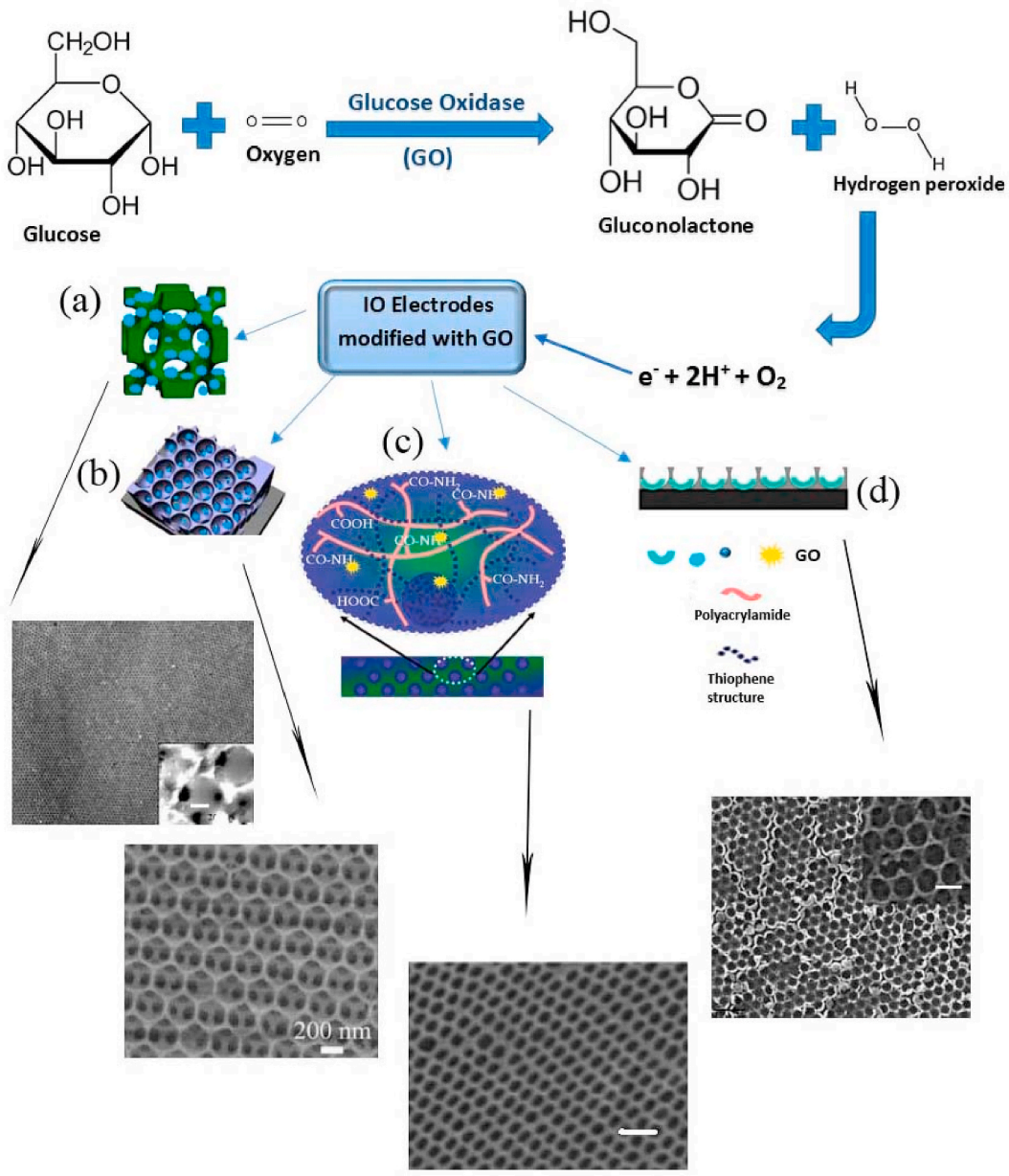

Fig. 4. Schematic images of glucose biosensors based IO: a) A schematic illustration and SEM image of the enzymatic ZnO IOs electrode b) schematic illustration and SEM image of ZnO IOPCs modified FTO electrode c) a schematic diagram and SEM image of IOs conducting hydrogel films d) A schematic illustration and SEM image of TiIOs film. Scale bar represented by 200 nm. Copyright 2013, AIP Publishing. Reproduced from Ref. [101]. Copyright 2014, Elsevier. Reproduced from Refs. [6]. Copyright 2012, Royal Society of Chemistry. Reproduced from Ref. [102]. Copyright 2008, John Wiley and Sons. Reproduced from Refs. [107]. IO: inverse opal, SEM: scanning electron microscopy, ZnO: zinc oxide, IOPCs: Inverse opal photonic crystals, FTO: fluorine-doped tin oxide.

changed through the ions produced by the catalytic activity of glucose, the optical response was produced and monitored by the blue shift of the reflection peak. To sense amperometric signals, the IOH films acted as a flexible electrochemical electrode to record current change. The optical and electrical results exhibited a reliable linear response for glucose detection (1–12 mM) and independent dual functions from developed IO conducting hydrogel film biosensor [102].

Titanium materials due to having optical features, pretty good electrical conductivity, and biocompatibility are extensively used in the fabrication of electrochemical and optical biosensors for the attachment of Abs or enzymes on the surface of sensors [103]. TiO_2 materials with different structural shapes and forms such as nanosheet, nanoparticles (NPs), nanofibers and recently 3D macroporous structures have found widespread applications in solar cells, photocatalysis, and lithium batteries [104–106]. Cao et al. have reported the enzymatic glucose biosensor based on 3D macroporous TiO_2 IO for the first time in 2008 [107]. They developed a face-centered cubic array of TiO_2 IO using sol-gel procedure and vertical deposition of PS colloidal crystals as opal templates. After modification of the ITO electrode surface with TiO_2 IO, GOX was immobilized on the surface of the sensor and the electrochemical of developed IO biosensor was characterized [107]. The results showed that the GOX/TiO_2 IO sensors compared with GO/TiO_2 electrodes have well-defined redox peaks and better sensitivity to the glucose concentration which is related to the great effective surface of the 3D ordered macroporous structure in designated TiO_2 IO (Fig. 4d).

The application of IOH as a colorimetric biosensor has been considered for the detection of biomolecules. In this regard, a unique and facile glucose detection method based on the IO polymer hydrogels was developed [108]. The vertical deposition method of SiO_2 microspheres was carried out for preparation of IOH structures, the opal

template was formed and then the mixture of acrylamidophenylboronic acid as a monomer, ethylene glycol dimethyl acrylate as cross-linking agent and azobis as a radical initiator was filled over the SiO_2 PC template. Finally, the polymerization was performed under UV irradiation [108]. The IOH structure was detected sugars with 1,2-cis-diol function and it is useful for naked-eye diagnosis of diabetes. Lee et al. employed the reversible swelling IOH film as a glucose-testing marker by photopolymerization of hydroxyethel methacrylate and phenylboronic acid [109]. The result shows that maximum diffraction response is related to the 6.25% phenylboronic acid hydrogel at 100 mM glucose which indicated IOH favorably swelled in the substrate usual direction. A reversible synthetic colorimetric glucose biosensor was developed using the IO polymer membrane confined with glucose-responsive hydrogel particles which that show specific color in 3D ordered arrays at visible light [110].

IOH based biosensors due to having unique polymer matrix in its structures are able to inhibit nonspecific binding during detection step. In addition, the polymer backbone by definite recognition units interact specifically with the related analyte molecules which led to an increase in sensitivity of IOH biosensors. Also, using biocompatible polymer materials of IOH, the analyte bioassays can be done under physiological conditions.

4.2. Protein detection

IO label-free materials are attractive and suitable sensing systems for the detection of proteins due to potency in portable POCT devices and color metric for visual biosensor applications. Based on the intuitive structural color of IOs, they could be used for the diagnosis of biological molecules without the need of sophisticated analysis instruments [111, 112].

A novel biosensor designed based on a combination of MIP and IO structures for selective detection of human serum albumin (HSA) [113]. For the preparation of MIP-IO structures, after the formation of SiO_2 microspheres PC, the bithiophene modified HSA was attached on the surface of SiO_2 using triethoxysilane linkers. Then, the potentiostatic polymerization of bithiophene led to the deposition of MIP film on the interspace of PC particles and after removing the SiO_2 microspheres and HSA, the polymeric IO structures were formed. The high affinity and selectivity of the developed biosensor are related to the exclusively HSA molecular cavities formed on the inner side of the hole wall. The femtomolar determination of HSA indicated the highly sensitive biosensor for the detection of HSA was developed using MIP due to its high specify and specific surface area (Fig. 5a) [113]. IOH based biosensor also was used for multiplexed protein study including capture Abs and a mixture of three heme proteins (Mb, Cyt C, and Hb) [114]. In this work, after the fabrication of IOH-beads, Abs were attached on IO structures by glutaraldehyde linker and then incubated with different concentrations of three heme proteins (Fig. 5b). Finally, the obtained protein-IOH was soaked in plasmonic Ag nanoparticles (Ag NPs) to intensify Raman signals from plasmonic staining. By the combination of the plasmonic materials like Ag NPs and PC materials, surface enhanced raman spectroscopy (SERS) analysis was provided for multiplex protein detection [114].

3D ordered macroporous TiO_2 IO have been used as label-free immunosensor for the detection of human IgG [82]. For the generation of microcavities structures, IO PMMA microspheres were self-assembled on a glass substrate. TiO_2 was infiltrated in interstitial space of the PMMA spheres as a target material and after removing the organic template by etching, IO structures were formed. The fabricated TiO_2 IO probes were used as a biosensor for reflectometry interference spectroscopy during the biomolecule detection. The antihuman IgG was immobilized directly on the void surface of IO by physical adsorption. This TiO_2 IO biosensor showed a sensitivity of 1 μg/mL (1.5 pg/mm^2) for IgG protein by monitoring the reflected signals and the shift of the diffraction peaks.

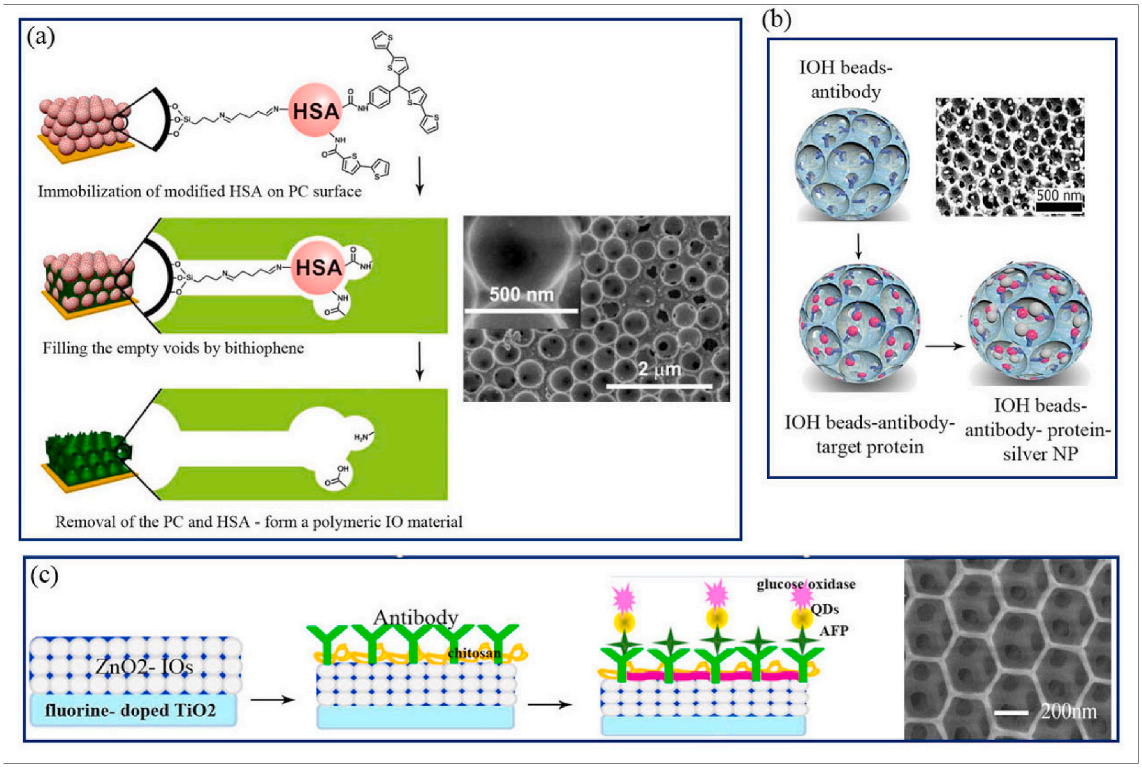

Fig. 5. a) Schematic diagram of IOs imprinting method for has detection b) illustration of photonic-plasmonic IOPHB for multiplexed analysis of proteins c) preparation processes of the ZnO IO immunosensor. Copyright 2017, Elsevier. Reproduced from Ref. [113]. Copyright 2015, John Wiley and Sons. Reproduced from Ref. [27]. Copyright 2015, Elsevier. Reproduced from Refs. [115]. HSA: Human serum albumin, IOs: Inverse opals, QDs: quantum dots.

Xu et al. have designed a photoelectrochemical biosensor based on ZnO IOs for the detection of alpha-fetoprotein (AFP) a liver cancer biomarker with LOD of 0.01 ng/mL [87]. In this work, ZnO IOs and quantum dots (QDs) were applied on the photoelectrochemical electrode surface. As seen in Fig. 5c, the Abs were immobilized on chitosan/fluorine-TiO_2/ZnO–IOs electrode surface and the composite of AFP-QDs-GOX were used as a tracer to enhance the sensitivity of immunosensor [87]. In the other work, they developed IO biosensor for detection of AFP using IOs–Ag_2S NPs [116]. The ZnO IO/Ag_2S composite led to the development of light absorption to long wavelengths. AFP was detected with LOD of 8 pg/mL which was almost 1.5 times better than the previous method. This result is related to effective matching of energy levels among the transmission bands of Ag_2S and ZnO IO which led to better photo-generated electrons conduction in ZnO IO/Ag_2S structures [116].

In addition to TiO_2 based IOs, IOH nonporous structures can be used for label-free and selective detection of the IgG Ab [117]. For the fabrication of IOH structures, PC film was formed by the dispersion droplet method of SiO2 microspheres [68]. Then the prepared PC films were immersed in a mixture of poly (ethylene glycol)-diacrylate and photoinitiator solution. After photo curable, a polyethylene terephthalate film was covered on the film. Finally, IOH arrays were shaped after exposition UV and wet etching of SiO_2 NPs (Fig. 6a) [117]. The color of fabricated IOH changed from green to orange with increasing the IgG concentration which can be detected by the naked eye and 50 nm band gap shift in absorbance spectra.

Enzymatic biocatalysts have the main role in accelerating (Table 1) chemical reactions in biological systems was also designated by IOs structures [118]. The immobilization of enzymes on the surfaces of specific carriers such as porous structures, ordered IOs arrays or pickering emulsion led to an increase in recovery and achieve a more activity, efficiency, and stability of the enzymes [119–121]. Fig. 6b shows a facile and promising approach for the fabrication of enzyme-based 3D IOs biocatalysts using the PC templating method. Horseradish peroxidase (HRP)-and amylase-based IOs were prepared using a filling of enzyme and bovine serum albumin (BSA) molecules into the voids of the PC template [122]. Free amino groups of BSA can increase the cross-linking efficiency, and thus facilitate in obtaining the enzyme-based IOs with high catalytic performance [123].

Wang et al. employed MNPs-tagged IOH as an enzymatic biocatalyst [125]. Due to having the huge surface regions in micro-pores of IOs the enzymes attachment and the efficiency of biocatalysts can be upgraded [126]. In this study, the fabrication process of IOH modified enzyme consist of several steps including 1) preparation of pregel solution (a mixture of the acrylamide, methylpropiophenone, and MNPs in water), 2) immersing of SiO_2 PC template in pregel, 3) polymerization by UV and removing the PC template by NaOH solution, and 4) activating the carboxylic groups and enzyme attachment by amine coupling method [125].

Using IOs immunsensor arrays for protein detections, a simple and effective method has been developed with high sensitivity, specificity, good regenerability, and durable stability. IOs structures using a wide internal surface of pores are able to physically bind of proteins on the nano-cavities surfaces [133]. Also, due to having the notable optical properties in IOs, the reflectance optical response and diffraction peak shift can be realized by the absorbing and increasing of proteins on the IOs pore surfaces [134]. So, developed IO immunosensors can be expanded for diagnosis of other biomarkers or pathogens with introducing a new route for label-free bio-sensing detection.

4.3. Virus detection

To protect the human body from viral infections, early detection of the virus using non-invasive, high sensitive and novel bio-sensing systems are extremely effective for maintaining human health. In this regard, optical detection based on PC biosensors for real-time observing of virus contamination may be useful than time-consuming pathogen-specific molecular detection approaches like polymerase chain reaction (PCR) and enzyme-linked immunosorbent assay (ELISA) [135]. Rapid and sensitive viral PC sensing methods that do not require labeling and multiple chemical modification processes have been applied to detect the intact virus particles in real test samples [136]. Endo T and colleagues in 2010 developed a reflectometric 2D PC biosensor for detection of influenza virus with LOD of 1 ng/mL in human saliva by immobilizing of Ab on the periodic structures of PC surface [137]. The developed PC biosensor was fabricated by nanoimprint lithography

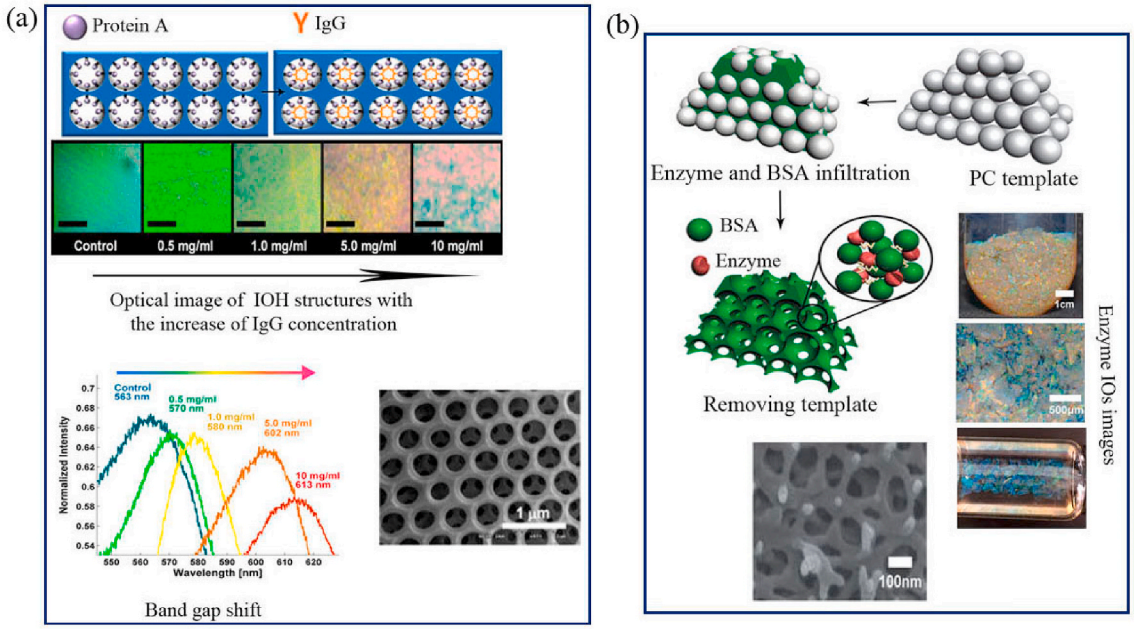

Fig. 6. a) Protein A immobilization and IgG binding to IOH structures,b) formation of enzyme-based IOs and related SEM images of IOs arrays. Copyright 2013, Elsevier. Reproduced from Ref. [111]. Copyright 2014, Royal Society of Chemistry. Reproduced from Ref. [124]. IOs: Inverse opals, IOPHB: Inverse opal photonic crystal hydrogel beads, IgG: Immunoglobulin G, IOH: Inverse opal hydrogel, SEM: scanning electron microscopy.

Table.1
Examples of some biological molecules (glucose, protein, virus and DNA) detection using IO based biosensors.

Bio-sensing method	IO material	A pore size	Detected target	LOD	General advantages	Ref.
Enzymatic	ZnO and NW	300 nm	Glucose	0.01–18 mM	Extended linear detection ranges and long-term stability	[101]
Enzymatic	TiO_2	300 nm	Glucose	151 μA cm-2 mM-1	Well-defined redox peaks	[107]
Colorimetric	Hydrogel	220 nm	Glucose	Not mentioned	Novel naked-eye detection of diabetes with multiple reuse	[112]
Enzymatic & Photo-electrochemical	ZnO	300 nm	Glucose	52.4 mA/mM cm^2	Improvement the sensor performance	[6]
Immunosensor	TiO_2	275 nm	IgG	1 μg/mL	Large internal surface area, low fluorescence background	[82]
Chemosensors	MIP film- SiO_2 NPs	500-nm	HSA	15- 150 fM	Developing the EG-FET transducer	[113]
Immunosensor & photoelectrochemical	ZnO & Ag_2S NPs	250 nm	AFP	8 pg/mL	Matching of energy levels between the conduction bands of Ag_2S and ZnO IO	[87]
Immunosensor	SiO_2 IO	263.6 ± 12.9 nm	*Influenza A H1N1* virus	10^3 to 10^5 PFU	Sensitively and selectively detection of H1N1 subtype	[127]
Immunosensor	Hydrogel	350 nm	*Rotavirus*	6.35 μgl/ml	Having more sensitivity for *Rotavirus* compare to ELISA	[128]
Apta sensor	SiO_2	370 nm	DNA	Not mentioned	Developing a reliable method for DNA-aptamer immobilization	[129]
DNA sensor	TiO_2-GNPs	200 nm	DNA	10 pM	Label-free DNA detection of SARS and HIV	[130]
DNA sensor	Hydrogel- QDs	260 nm	DNA	1 nM	Developing multiplexing label-free DNA detection	[131]
DNA sensor	SiO_2 and Ag nano sheet	460 nm	DNA	5 nM	Reporting a facile strategy to preparation SERS-active substrate	[132]

NW: nanowire; IOH: invers opal hydrogel, MIP: molecularly imprinted polymer, EG-FET: extended-gate field-effect transistor; PFU: plaque forming unit, AFP: alpha-fetoprotein, GNPs: Gold nanoparticles, QDs: Quantum Dots; SARS: severe acute respiratory syndrome; HIV: human immunodeficiency virus; SERS: Surface enhanced Raman spectroscopy. IOs: Inverse opals, IgG: Immunoglobulin G, HSA: Human serum albumin, ELISA: enzyme-linked immunosorbent assay, H1N1: influenza virus.

(NIL) which defined as a method for the production of nanometer-scale 2D arrays with high reproducibility [138,139].

Influenza A virus (*H1N1*) which defined as a cause of acute infectious disease and a serious public health hazard, was sensitively and selectively monitored using developed SiO_2 IO [127]. In this study, nanostructures of SiO_2-based IOs were fabricated by vertical immersion of silicon substrate in the colloidal PS and a tetraethyl orthosilicate (TEOS) suspension [140]. After Ab immobilization on the SiO_2 surface, the *H1N1* virus was detected by the redshift reflectance spectra without complex labeling processes. Developed 3D SiO_2 IO with possessing the bulky surface of the cavities and well organized optical properties, exhibited high sensitivity in the range of 10^3–10^5 plaque forming unit (PFU) and high specificity to the H1N1 virus [127].

In other work, a direct label-free biosensor was developed based on 3D PC hydrogel IOs for the detection of *Rotavirus* [128]. Developed IOs biosensor has the potential to apply in the POCT due to having simple, cost-effective fabrication and high sensitivity for intact virus detection. For fabrication of IOHs, colloidal SiO_2 nanospheres (350 nm) used as a template and then ethylene glycol diacrylate and polyethylene terephthalate films were applied for making hydrogel backbone. After UV exposing, wet and O_2 plasma etching the SiO2 template, the IOs structures were obtained for virus impregnation [111,128]. Anti-Rotavirus IgG was immobilized on the surface of hydrogel (ethylene glycol diacrylate) through the chemical binding. An optical spectrum analyzer was used for sensing virus attachment on the modified surface using shifting in peak wavelength value. This IOs biosensor can monitor the target with a virus sample from 6.35 μg/mL to 1.27 mg/mL without the pretreatment process.

A label-free biosensor based on PC structures was designated for the detection of viable *Rotaviruses* [136]. The PC surface was fabricated on the bottom surface of each well in plastic microplates which comprised a 1D periodic structure of a low refractive index polymer with a high refractive index of TiO_2 film. The combination of the PC biosensor onto 96 or 384 microplate wells permits for parallel quantification of various screening of viruses contaminants in water samples without the use of further label reagents [136,141].

4.4. DNA detection

Today, PC based biosensors with periodical structures have been introduced for the detection of DNA sequences due to having optical features like PBG [81,142]. The unique properties of PCs biosensors make them as a novel method to intensifying responses to develop highly sensitive photonic biosensors. For example, an effective detection method was presented using fluorescence resonance energy transfer (FRET) and PC optical signal for DNA hybridization detection [1]. The polymer microspheres including PS, polymethyl methacrylate, and polyacrylic acid were used for the self-assembling of PCs structures (Fig. 7a). This developed DNA biosensor by fluorescein-labeled DNA molecules and ethidium bromide was able to detect the single-mismatch probes with a sensitivity of 13.5 fM [1]. Also, PCs structures were used for the detection of Alzheimer's disease by monitoring a DNA oligonucleotide sequence in the apolipoprotein E4 gene [142]. 2D-PCs biosensor was fabricated by a printable photonics method and coating localized-surface plasmon resonance (LSPR) gold layer on 2D-PC surfaces. DNA oligonucleotide probe was detected not only using decreasing in reflectance of PCs structures but also monitored by decreasing in LSPR responses on Au-coated PCs surfaces (Fig. 7b).

Chiappini and colleagues designed and fabricated DNA aptasensor using single-stranded DNA sequences and the SiO_2 IOs [129]. The immobilization of DNA molecules to Cy3 fluorophore was done on the IOs surfaces after the functionalization of the SiO_2 hollow spheres via trimethoxysilane epoxy-chemistry. The formation of a covalent bond between the amino-modified DNA-aptamer and epoxy IOs surface makes a reliable and effective approach for coating the entire thickness of IO networks using DNA-dye labeled fluorescence systems [129].

In 2010, a low-cost, simple and label-free of suspension biosensor arrays for detecting DNA variations and genetic probes were provided by quantum dot (QD) and IO hydrogels [131]. The related signals for quantitatively monitoring of DNA hybridization in microcarrier hydrogel arrays were detected by the blue shift in the Bragg diffraction peak location with LOD of 1 nM. For the preparation of hydrogel photonic beads, the SiO_2 colloidal microspheres with a diameter of 260 nm were used as a template and then immersed in the hydrogel solution, which composed of acrylamide, acryloyl-modified ssDNA and photoinitiator

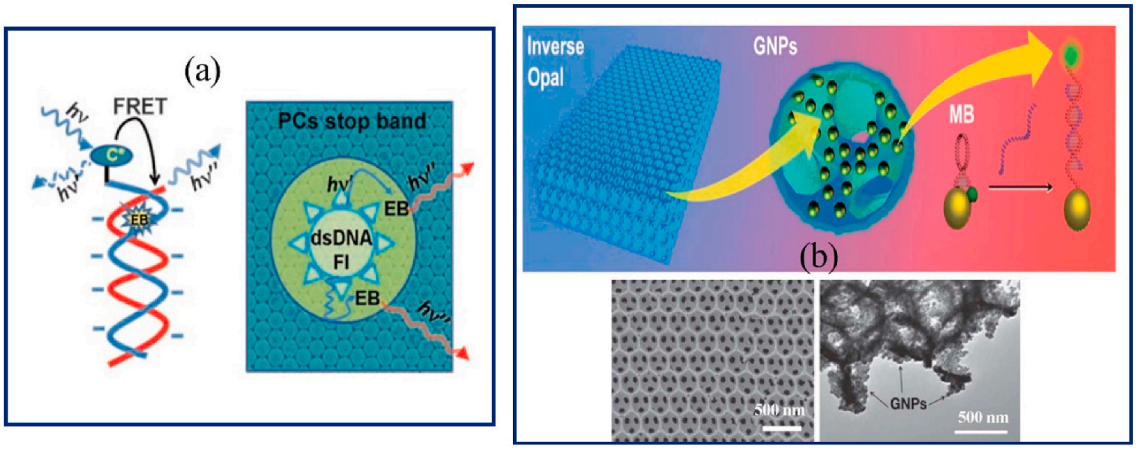

Fig. 7. a) DNA sequence detection based on a FRET mechanism and effect of the PC on FRET; b) Schematic illustration of the Au IO used for label-free detection of DNA. The detection system is composed of a TiO_2 IO, GNPs and labeled molecular beacons and related SEM image for TiO_2 IOs and after GNPs sputtering on the TiO_2 IOs surface. Copyright 2008, John Wiley and Sons. Reproduced from Ref. [143]. Copyright 2012, Royal Society of Chemistry. Reproduced from Ref. [81].

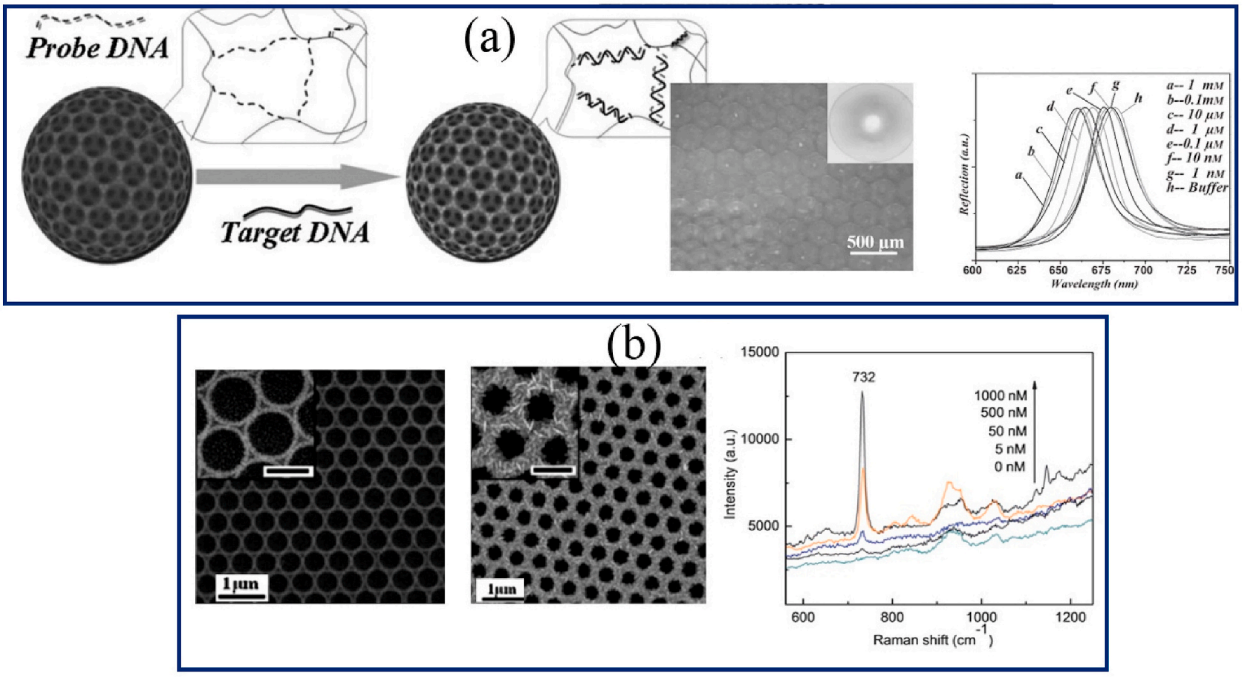

Fig. 8. a) Schematic diagram of the DNA detection by hydrogel-IOs, DNA-responsive hydrogel IOs (bright-field microscopic images) and the optical response of the DNA-responsive hydrogel photonic beads incubated in their corresponding target DNA with different concentrations; b) GNPs-assembled SiO_2 IOs film and 2D AgNS-coated IOs. The SERS spectra of the 2D AgNS-coated IOs treated with different concentrations of ssDNA solutions. Copyright 2010, John Wiley and Sons. Reproduced from Ref. [131]. Copyright 2012, Royal Society of Chemistry. Reproduced from Ref. [149]. EB: Ethidium bromide, FRET: Fluorescence resonance energy transfer, Fl: fluorescein, PC: Photonic crystal, DNA: Deoxyribonucleic acid, IO: Inverse opal, MBs: Molecular beacons, TiO_2: Titanium oxide, SEM: Scanning electron microscopy, GNPs: Gold nanoparticles, AgNS: Silver nanosheet, SERS: Surface enhanced Raman spectroscopy, ssDNA: single strand DNA. (For interpretation of the references to color in this figure legend, the reader is referred to the Web version of this article.)

(Fig. 8a). Finally, the DNA-responsive hydrogel photonic beads immersed in QDs solution for incorporation [131].

In addition to the application of QDs nanostructures in the construction of IOs, gold nanoparticles (GNPs) were used too in 3D-IOs structures for highly-sensitive DNA sequences detection in severe acute respiratory syndrome (SARS) and the human immunodeficiency virus (HIV) with LOD of 10 pM [130]. The use of PCs and plasmonic materials together in DNA biosensor structures made a remarkable and effective light harvesting. PCs structures in IOs were able to intensify the LSPR of GNPs when the wavelength of bandgap in PCs is near the LSPR absorption of the GNPs [130]. The TiO_2– Au IOs were fabricated by removing a microsphere opal template and sputtering of GNPs onto the IOs surfaces [145]. Also, a new kind of surface-enhanced Raman spectroscopy (SERS) substrates composed of 2D silver nanosheets and SiO_2 IOs was used for ultra-sensitive detection of rhodamine 6G and DNA sequence with LOD of 10 fM and 5 nM respectively [146]. After the preparation of SiO_2 IOs on the PS microsphere template, it was immersed in GNPs suspension for immobilization of GNPs on IOs surface (Fig. 8b). Then the gold surface was coated by silver nanosheets through the soaking films in the $AgNO_3$ solution. Having a high Raman enhancement feature in the d 2D silver nanosheet-IOs compare with silver membranes or uniform silver nanoparticle-coated substrates can

be utilized as a SERS-active film for ultra-sensitive detection systems of bimolecular [132,147,148]. With a reducing DNA concentration, the intensity of Raman peak related to adenine (in 732 cm^{-1}) slowly reduces indicating the resultant IOs based DNA biosensor is suitable for label-free detection.

Using IOs structures, the simple and effective platforms to sense the DNA hybridization was introduced in the clinical detection of biomolecules, food adulteration, environmental analysis, and so on [4,150,151]. For detection of the low abundance of DNA, several conventional techniques have been made like Northern Blotting, polymerase chain reaction (PCR) and microarrays which involved amplification steps with labeled enzymes, fluorophore probe or tagged-nanoparticle [152]. These techniques are intrinsically complex, time-consuming and require multiple layers of interacting components with high specificity [153]. Therefore, for the genetic and pathogenic infection diagnosis, it is needed to design the facile, powerful, highly sensitive and label-free DNA detection methods.

Biosensors based on the IO chips for DNA detection have some advantages compared with traditional methods including small sample volume needed, label-free detection, availability of sensors, rapid detection, reusable sensor chips and portability which provided them for use in POCT device. Also, IOs based biosensors for DNA detection have more potential in early discovery of cancer disease. For example low amount of miRNA detection was provided by periodic PC structures in cancer cells [154].

4.5. Other bio-molecules detection

The POCT bio-sensing devices based IO materials are capable of measuring disease-related factors like bacteria toxin, cholesterol, creatinine, etc. in blood or urine with the minimal extent of sample and reagent (Table 2) [87,155]. A sensitive multiple bacteria biosensor for *Escherichia coli* and *Staphylococcus aureus* detection using magnetic-IOH based biosensors was introduced by Xu et al. with LOD of 100 CFU/mL [156]. IOH structures were made by filling of poly (ethyleneglycol) diacrylate and acrylic acid pregel solution into the voids of SiO2 PC beads. After the polymerizing of pregel by UV light and removing the SiO_2 PC template with hydrofluoric acid, the IOH beads were saturated in MNPs. As seen in Fig. 9a the surface of magnetic-IOH beads was coated by specific aptamer probes and the attached bacteria on the IOH surface was separated magnetically after several hours incubation in infected blood [156].

In the work by Zhao et al. the creatinine was detected in artificial urine samples with LOD of 0.9 mg/dL using IOs nanostructured capillary tubes in the combination of enhanced surface Raman of GNPs [157]. For this purpose, the mixture of PS and SiO_2 nanopheres were infiltrated by self-assembly into the capillaries, after calcination, the capillary-IOs structures were fabricated. Fig. 9b illustrates the capillary-IOs fabrication steps. The GNPs were synthesized in situ in the nano-holes of the capillary-IOs for the functionalization of capillary-IOs at SERS analysis [157]. The cholesterol concentration which is related to coronary heart disease was detected by a nonenzymatic CIOs based biosensor [158]. The usual range of total cholesterol in human serum blood is 1.3–2.6 mg/mL and developed CIOs biosensor can detect 0.5 mg/mL cholesterol in several minutes. The rod shape of CIOs was prepared by self-assembly of SiO_2 nano-spheres in the capillary using the solvent evaporation method and dipping the PC-capillary in carbon precursor solution contains ethanol, sucrose, water, and H_2SO_4 (Fig. 9c). After immersing rod shape of CIOs in the cholesterol samples, the shifts in reflection peak of CIOs showed high linear relation with cholesterol ranges [158].

TiO_2 IOs were used for sensitive detection of H_2O_2 (70.04 μA/mM) using immobilization HRP on the electrode surface [80]. in photo-enhanced TiO_2 IOs biosensors, the highly 3D ordered, macroporous and nanometer-scale organizations can lead to the excellent photovoltaic effect and performance [80].

Generally, alcohol meter was applied for detection of the ethanol concentration in the distilled liquors which are based on the shift in the refractive index the samples containing alcohol. Also, SPR based biosensors can evaluate the ethanol concentration exactly but its device and operation procedure is high expensive and complicated [161]. These limitations have led researchers to develop simple, inexpensive, and high-sensitivity biosensors. Recently, SiO_2 and TiO_2 IO biosensors have been fabricated as the optical or chemical biosensors to sense the different amounts of ethanol using the monitoring of peak positions shift in the reflectance spectra [1,160]. The obtained results showed that the 3D nanoporous of TiO_2 IO films have the perfect optical properties and higher sensitivity in comparison with SiO_2 IO biosensors for quantitative detection of the ethanol concentration which reaches to 10% difference ($v/v0$). Hu et al. developed an ultrasensitive imprinted photonic polymer biosensor with IOs structures for label-free detection of theophylline with LOD of 0.1 fM [162]. In this study, the SiO_2 colloidal crystal was used for PC template and theophylline was applied as template molecules for the molecular-imprinting method.

Having the perfect optical properties and higher sensitivity in TiO_2 for detection of biomolecules are related to the higher refractive index and good hydrophilic surface of the developed TiO_2 IOs optical biosensors. Also, developing IOs biosensors for biomolecules detection can be supported the in vitro bio-transformations for different types of enzymatic reaction studies. Mainly, for macromolecular substrates, this porous IOs biocatalyst structures can reduce mass transfer resistance significantly. Moreover, the macro-pore size and morphology of enzyme-based IOs can be easily controlled by the size of polymer microspheres in colloidal PC templates.

5. Advantages of IOs biosensors

Numerous optical approaches has been used for detection biomarkers including SPR, LSPR, waveguide structures, and fluorescence transfer [163–166]. The advent of novel biosensor-based technologies like optic-based sensing methods contributes to a precise diagnosis. Among the different types of optical systems, PCs have attracted considerable attention because of their unique optical features [167]. Due to the size controlling of the colloidal crystal microsphere in the template, this methodology was introduced as a feasible and significant

Table.2
Examples of some biological elements detection using IO based biosensors.

Bio-sensing method	IO material	A pore size	Detected target	LOD	General advantages of developed IO	Ref.
Photoelectrochemical	TiO_2	300 nm	H_2O_2	70.04 A/mM	Excellent photoelectrical property and the large effective surface	[80]
Nonenzymatic	CIORs	222 nm	Cholesterol	0.5 mg/mL	UV–vis spectrometer	[158]
Aptasensor	Hydrogel	200–300 nm	Bacteria	100 CFU/mL	Rapid and sensitive detection for hematological infections	[156]
Optical	TiO_2 Or SiO2	223–273 nm	Ethanol	Not mentioned	Being useful for detecting the ethanol	[160]
Optical	SiO_2IO-capillaries	260 nm	Creatinine	0.9 mg/dL.	Making nanostructured capillary tubes for SERS analysis in a flow-through fashion.	[87]

NW: nanowire; SERS: Surface enhanced Raman spectroscopy. IOs: Inverse opals, CIORs: carbon inverse opal rods, CFU: colony-forming unit.

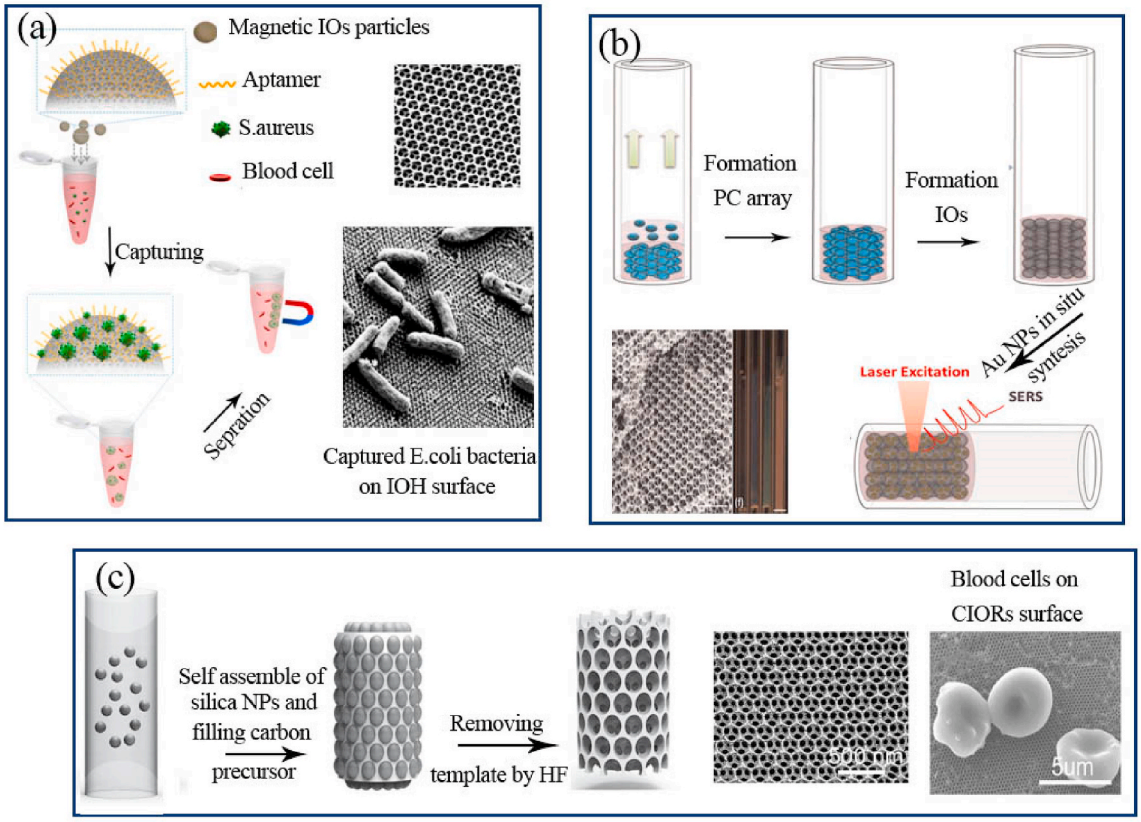

Fig. 9. a) Illustration of magnetic IOH fabrication steps with aptamer probes for the bacteria detection b) schematic fabrication of GNPs incorporated capillary IOs for SERS in creatinine biosensor c) the preparation of rod shape of CIOs for cholesterol detection. Copyright 2018, Elsevier. Reproduced from Ref. [159]. Copyright 2015, Elsevier. Reproduced from Refs. [87]. Copyright 2015, John Wiley and Sons. Reproduced from Ref. [158]. GNPs: gold nanoparticles, IOH: Invers opal hydrogel, IOs: Invers opals, SERS: Surface enhanced Raman spectroscopy, CIOs: Carbon inverse opals. (For interpretation of the references to color in this figure legend, the reader is referred to the Web version of this article.)

IOs synthesis in the numerous related laboratory. The periodicity, size and refractive index of PCs are responsible for the specific optical properties of PCs structures which is controllable by nano-imprint lithography (NIL) technology used for fabrication of IOs biosensors [168,169].

Common techniques for detection of biomarkers like ELISA or PCR which are less flexible, tedious/laborious assay, and expensive method with an inadequate range of sensitivity for detection of biological markers [170]. Among them, label-free detection systems acts in their natural forms and are based on the probe of binding-induced refractive index changes. For the biosensor uses, the IOs platforms displayed some distinct advantages. One was the unique light guiding system of the IOs arrays, which ensured a strong light-matter interaction. The other is related to the strictly packed sphere-shaped air holes arranged in a cubic-closest-packed lattice of IOs structures. These nano-holes which are able to save nano volume of fluidic biological samples can act as a simple fluidic channel to inject the substances during sensing process. An important advantage of biological fluid filled in IOs structures is its ability for sensitive label-free detection. In IOs based biosensors, simple and energy-efficient production method with high amount of sensitivity make them attractive systems for optical sensing uses. For example, in preparation sol-gel process of silica IOs structures infiltration of the initial direct opal template was done in low temperature which led to produce the high-quality periodic arrays of silica. High thermal and chemical strength of silica glass allows performance of optical detection in an extensive temperature range with different fluidic environments [12].

Compared with other optical biosensors like SPR based bioassays, the IOs structures show the higher environmental sensitivity. Finally, designing the IO biosensors with various filling materials like TiO_2, ZnO, SiO_2 and hydrogel polymers due to having the large surface area of nano-pores with the 3D nanostructure compared with current optical based biosensors, enables them to mix with microfluidics and lab-on-a chip tools to develop the sensor for POCT sensing applications. In addition, numerous sensing approaches can be applied via the various surface modification methods for detection of biological markers. Also, the nano-to femto-molar limit of detection using IO based biosensors can be more employed for the detection of various biomarkers.

6. Conclusions and future perspectives

This review presents some recent advances that focus on the IOs structures and their applications as optical biosensors. The novel, facile, sensitive, and label-free bio-sensing systems with quick responses are essential for POCT and health-related sensing devices. Remarkable developments in the synthesis of IOs based biosensors have been achieved in recent years, suggesting their potential as an optical clinical diagnostic tool. IOs structures provided by several kinds of material including TiO_2, ZnO, polymeric hydrogel, SiO_2 or metallic NPs have an ideal opportunity for the development of versatile biosensor platforms with superior characteristics. The label-free detection of IO-based biosensors and its high surface-to-volume ratio, which is related to the nano and microporous IOs structures, along with simple and available optical diagnostic devices, definitely in the future they will become more compact and efficient bio-sensing tools in the POCT systems and health service market.

Declaration of competing interest

The authors declare that they have no known competing financial interests or personal relationships that could have appeared to influence the work reported in this paper.

Acknowledgements

The authors are grateful for financial support from Ardabil University of Medical Sciences (Grant No: IR.ARUMS.REC.1398.627) and Iran National Science Foundation (INSF).

References

[1] J. Li, T. Zheng, A comparison of chemical sensors based on the different ordered inverse opal films, Sensor. Actuator. B Chem. 131 (1) (2008) 190–195.
[2] G. Sancho-Fornes, M. Avella-Oliver, J. Carrascosa, E. Fernandez, E.M. Brun, Á. Maquieira, Disk-based one-dimensional photonic crystal slabs for label-free immunosensing, Biosens. Bioelectron. 126 (2019) 315–323.
[3] F. Fathi, R. Rahbarghazi, M.-R. Rashidi, Label-free biosensors in the field of stem cell biology, Biosens. Bioelectron. 101 (2018) 188–198.
[4] M. Mansouri, B. Khalilzadeh, A. Barzegari, S. Shoeibi, S. Isildak, N. Bargahi, Y. Omidi, S. Dastmalchi, M.-R. Rashidi, Design a Highly Specific Sequence for Electrochemical Evaluation of Meat Adulteration in Cooked Sausages, Biosens. Bioelectron, 2019, p. 111916.
[5] P. Chaghamirzaei, D. Raeyani, A. Khosravi, S. Allahveisi, B. Abdollahi-Kia, F. Bayat, B. Olyaeefar, S. Ahmadi-Kandjani, Real-time detection of gas and chemical vapor flows by silica inverse-opals, IEEE Sensor. J. 19 (18) (2019) 7961–7967.
[6] L. Xia, J. Song, R. Xu, D. Liu, B. Dong, L. Xu, H. Song, Zinc oxide inverse opal electrodes modified by glucose oxidase for electrochemical and photoelectrochemical biosensor, Biosens. Bioelectron. 59 (2014) 350–357.
[7] P.S. Pakchin, H. Ghanbari, R. Saber, Y. Omidi, Electrochemical immunosensor based on chitosan-gold nanoparticle/carbon nanotube as a platform and lactate oxidase as a label for detection of CA125 oncomarker, Biosens. Bioelectron. 122 (2018) 68–74.
[8] P.S. Pakchin, M. Fathi, H. Ghanbari, R. Saber, Y.J.B. Omidi, A novel electrochemical immunosensor for ultrasensitive detection of CA125 in ovarian cancer, Biosens. Bioelectron, 2020, p. 112029.
[9] S. John, Strong localization of photons in certain disordered dielectric superlattices, Phys. Rev. Lett. 58 (23) (1987) 2486.
[10] H. Altug, J. Vučković, Polarization control and sensing with two-dimensional coupled photonic crystal microcavity arrays, Opt. Lett. 30 (9) (2005) 982–984.
[11] F. Bayat, S. Ahmadi-Kandjani, H. Tajalli, Designing real-time biosensors and chemical sensors based on defective 1-D photonic crystals, IEEE Photon. Technol 28 (17) (2016) 1843–1846.
[12] Y. Nishijima, K. Ueno, S. Juodkazis, V. Mizeikis, H. Misawa, T. Tanimura, K. Maeda, Inverse silica opal photonic crystals for optical sensing applications, Optic Express 15 (20) (2007) 12979–12988.
[13] Q. Li, S. Zhou, T. Zhang, B. Zheng, H. Tang, Bioinspired Sensor Chip for Detection of miRNA-21 Based on Photonic Crystals Assisted Cyclic Enzymatic Amplification Method, Biosens. Bioelectron, 2019, p. 111866.
[14] X. Fan, I.M. White, S.I. Shopova, H. Zhu, J.D. Suter, Y. Sun, Sensitive optical biosensors for unlabeled targets: a review, Anal. Chim. Acta 620 (1–2) (2008) 8–26.
[15] E. Yablonovitch, Inhibited spontaneous emission in solid-state physics and electronics, Phys. Rev. Lett. 58 (20) (1987) 2059.
[16] U. Grüning, V. Lehmann, C. Engelhardt, Two-dimensional infrared photonic band gap structure based on porous silicon, Appl. Phys. Lett. 66 (24) (1995) 3254–3256.
[17] A. Blanco, E. Chomski, S. Grabtchak, M. Ibisate, S. John, S.W. Leonard, C. Lopez, F. Meseguer, H. Miguez, J.P. Mondia, Large-scale synthesis of a silicon photonic crystal with a complete three-dimensional bandgap near 1.5 micrometres, Nature 405 (6785) (2000) 437–440.
[18] M. Chhabra, C. Selwal, Design of a Photonic Crystal Biosensor Using DNA Filled Microcavity and Ring Cavity Coupled with Waveguide, in: International Conference on Signal Propagation and Computer Technology (ICSPCT 2014), IEEE, 2014, pp. 342–345.
[19] Y.-C. Hsiao, Hybrid liquid-crystal/photonic-crystal devices: current research and applications, Photonic Crystals-A Glimpse of the Current Research Trends, IntechOpen2019.
[20] M.Y. Azab, M.F.O. Hameed, A.M. Nasr, S. Obayya, Multifunctional Plasmonic Photonic Crystal Fiber Biosensors, Computational Photonic Sens, Springer2019, pp. 233-260.
[21] A.E. Cetin, S.N. Topkaya, Photonic crystal and plasmonic nanohole based label-free biodetection, Biosens. Bioelectron. 132 (2019) 196–202.
[22] G.I. Waterhouse, M.R. Waterland, Opal and inverse opal photonic crystals: fabrication and characterization, Polyhedron 26 (2) (2007) 356–368.
[23] J. Divya, S. Selvendran, A.S. Raja, Photonic crystal-based optical biosensor: a brief investigation, Laser Phys. 28 (6) (2018), 066206.
[24] E. Armstrong, C. O'Dwyer, Artificial opal photonic crystals and inverse opal structures–fundamentals and applications from optics to energy storage, J. Mater. Chem. 3 (24) (2015) 6109–6143.
[25] B. Cunningham, M. Zhang, Y. Zhuo, L. Kwon, C. Race, Review of recent advances in biosensing with photonic crystals, IEEE Sensor. J. 16 (10) (2014) 3349–3366.
[26] H. Inan, M. Poyraz, F. Inci, M.A. Lifson, M. Baday, B.T. Cunningham, U. Demirci, Photonic crystals: emerging biosensors and their promise for point-of-care applications, Chem. Soc. Rev. 46 (2) (2017) 366–388.
[27] Z. Mu, X. Zhao, Y. Huang, M. Lu, Z. Gu, Photonic crystal hydrogel enhanced plasmonic staining for multiplexed protein analysis, Small 11 (45) (2015) 6036–6043.
[28] W.S. Lee, T. Kang, S.-H. Kim, J. Jeong, An antibody-immobilized silica inverse opal nanostructure for label-free optical biosensors, Sensors 18 (1) (2018) 307.
[29] G. Chen, K. Zhang, B. Luo, W. Hong, J. Chen, X. Chen, Plasmonic-3D photonic crystals microchip for surface enhanced Raman spectroscopy, Biosens. Bioelectron. 143 (2019) 111596.
[30] F. Bayat, P. Chaghamirzaei, A. Nikniazi, S. Ahmadi-Kandjani, M.-R. Rashidi, H. Tajalli, Optimizing the concentration of colloidal suspensions in convective assembly of centimeter-sized uniform monolayer colloidal crystals, Appl. Surf. Sci. 434 (2018) 898–904.
[31] M. Sawangphruk, J.S. Foord, Permselective properties of polystyrene opal films at diamond electrode surfaces, Phys. Chem. Chem. Phys. 12 (28) (2010) 7856–7864.
[32] S.G. Johnson, J. Joannopoulos, Three-dimensionally periodic dielectric layered structure with omnidirectional photonic band gap, Appl. Phys. Lett. 77 (22) (2000) 3490–3492.
[33] G. Guida, A. De Lustrac, A.C. Priou, An introduction to photonic band gap (PBG) materials, Prog. Electromagn. Res. 41 (2003) 1–20.
[34] E. Yablonovitch, Photonic crystals: semiconductors of light, Sci. Am. 285 (6) (2001) 46–55.
[35] B.T. Cunningham, Photonic Crystal Defect Cavity Biosensor, Google Patents, 2006.
[36] S.M. Shamah, B.T. Cunningham, Label-free cell-based assays using photonic crystal optical biosensors, Analyst 136 (6) (2011) 1090–1102.
[37] H.-B. Sun, S. Matsuo, H. Misawa, Three-dimensional photonic crystal structures achieved with two-photon-absorption photopolymerization of resin, Appl. Phys. Lett. 74 (6) (1999) 786–788.
[38] W. Zhang, N. Ganesh, I.D. Block, B.T. Cunningham, High sensitivity photonic crystal biosensor incorporating nanorod structures for enhanced surface area, Sensor. Actuator. B Chem. 131 (1) (2008) 279–284.
[39] A. Vinogradov, A. Dorofeenko, S. Erokhin, M. Inoue, A. Lisyansky, A. Merzlikin, A. Granovsky, Surface state peculiarities in one-dimensional photonic crystal interfaces, Phys. Rev. B 74 (4) (2006), 045128.
[40] Q. Zhao, Y. Wang, H. Cui, X. Du, Bio-inspired sensing and actuating materials, J. Mater. Chem. 7 (22) (2019) 6493–6511.
[41] S. Lis, R. Dylewicz, J. Myśliwiec, A. Miniewicz, S. Patela, Quick and Non-invasive Method for Characterisation of Profiles of Nano-Photonics Structures, Photonic Crystal Materials and Devices VIII, International Society for Optics and Photonics, 2008, p. 698917.
[42] S. Vignolini, E. Moyroud, B.J. Glover, U. Steiner, Analysing photonic structures in plants, J. R. Soc. Interface 10 (87) (2013) 20130394.
[43] S. Yoshioka, S. Kinoshita, Effect of macroscopic structure in iridescent color of the peacock feathers, FORMA-TOKYO- 17 (2) (2002) 169–181.
[44] P. Vukusic, J.R. Sambles, Photonic structures in biology, Nature 424 (6950) (2003) 852.
[45] J. Teyssier, S.V. Saenko, D. Van Der Marel, M.C.J.N.c. Milinkovitch, Photonic crystals cause active colour change in chameleons, Nat. Commun. 6 (2015) 6368.
[46] S. Das, N. Shanmugam, A. Kumar, S.J.B. Jose, Potential of biomimicry in the field of textile technology, Bioinspir. Biomim. Nan. 6 (4) (2017) 224–235.
[47] S. Kubo, A. Fujishima, O. Sato, H.C. Segawa, Anisotropic accelerated emission of the chromophores in photonic crystals consisting of a polystyrene opal structure, J. Phys. Chem. 113 (27) (2009) 11704–11711.
[48] P. Chaghamirzaei, D. Raeyani, A. Khosravi, S. Allahveisi, B. Abdollahi-Kia, F. Bayat, B. Olyaeefar, S.J.I.S.J. Ahmadi-Kandjani, Real-time detection of gas and chemical vapor flows by silica inverse-opals, IEEE Sensor. J. 19 (18) (2019) 7961–7967.
[49] E. Armstrong, W. Khunsin, M. Osiak, M. Blömker, C.M.S. Torres, C.J.S. O'Dwyer, Ordered 2D colloidal photonic crystals on gold substrates by surfactant-assisted fast-rate dip coating, Small 10 (10) (2014) 1895–1901.
[50] M. Holgado, F. Garcia-Santamaria, A. Blanco, M. Ibisate, A. Cintas, H. Miguez, C. Serna, C. Molpeceres, J. Requena, A.J.L. Mifsud, Electrophoretic deposition to control artificial opal growth, Langmuir 15 (14) (1999) 4701–4704.
[51] D. Agarwal, R. Chauhan, A. Kumar, D. Kabiraj, F. Singh, S. Khan, D. Avasthi, J. Pivin, M. Kumar, J. Ghatak, Synthesis and characterization of ZnO thin film grown by electron beam evaporation, J. Appl. Phys. 99 (12) (2006) 123105.
[52] W. Tang, D. Cameron, Aluminum-doped zinc oxide transparent conductors deposited by the sol-gel process, Thin Solid Films 238 (1) (1994) 83–87.
[53] H. Nanto, T. Minami, S. Shooji, S. Takata, Electrical and optical properties of zinc oxide thin films prepared by rf magnetron sputtering for transparent electrode applications, J. Appl. Phys. 55 (4) (1984) 1029–1034.
[54] M. Scharrer, A. Yamilov, X. Wu, H. Cao, R.P. Chang, Ultraviolet lasing in high-order bands of three-dimensional ZnO photonic crystals, Appl. Phys. Lett. 88 (20) (2006) 201103.
[55] M. Scharrer, X. Wu, A. Yamilov, H. Cao, R.P. Chang, Fabrication of inverted opal ZnO photonic crystals by atomic layer deposition, Appl. Phys. Lett. 86 (15) (2005) 151113.

[56] H. Yan, Y. Yang, Z. Fu, B. Yang, L. Xia, S. Fu, F. Li, Fabrication of 2D and 3D ordered porous ZnO films using 3D opal templates by electrodeposition, Appl. Phys. Lett. 7 (11) (2005) 1117–1121.

[57] X.-b. Lin, Y.-z. Zhao, J. Li, Q.-y. Hu, S.-j. Jiang, Z.-g. Cai, B.-j. Li, Fabrication techniques of inverse opal structure photonic crystal [J], J. Synth. Cryst. 6 (2004).

[58] V. Abramova, A. Sinitskii, Large-scale ZnO inverse opal films fabricated by a sol–gel technique, Superlattice. Microst. 45 (6) (2009) 624–629.

[59] K.-M. Huang, C.-L. Ho, H.-J. Chang, M.-C. Wu, Fabrication of inverted zinc oxide photonic crystal using sol–gel solution by spin coating method, Nanoscale Res. Lett. 8 (1) (2013) 306.

[60] G. Collins, E. Armstrong, D. McNulty, S. O'Hanlon, H. Geaney, C. O'Dwyer, 2D and 3D photonic crystal materials for photocatalysis and electrochemical energy storage and conversion, Sci. Technol. Adv. Mat. 17 (1) (2016) 563–582.

[61] J. Schneider, M. Matsuoka, M. Takeuchi, J. Zhang, Y. Horiuchi, M. Anpo, D. W. Bahnemann, Understanding TiO2 photocatalysis: mechanisms and materials, Chem. Rev. 114 (19) (2014) 9919–9986.

[62] X. Feng, K. Shankar, M. Paulose, C.A. Grimes, Tantalum-doped titanium dioxide nanowire arrays for dye-sensitized solar cells with high open-circuit voltage, Angew. Chem. Int. Ed. 48 (43) (2009) 8095–8098.

[63] H.C. Achterberg, L. Sørensen, F.J. Wolters, W.J. Niessen, M.W. Vernooij, M. A. Ikram, M. Nielsen, M. de Bruijne, The value of hippocampal volume, shape, and texture for 11-year prediction of dementia: a population-based study, Neurobiol. Aging 81 (2019) 58–66.

[64] P. Jiang, J. Bertone, K. Hwang, V. Colvin, Single-crystal colloidal multilayers of controlled thickness, Chem. Mater. 11 (8) (1999) 2132–2140.

[65] J. Zhang, Z. Sun, B. Yang, Self-assembly of photonic crystals from polymer colloids, Curr. Opin. Colloid Interface Sci. 14 (2) (2009) 103–114.

[66] S. Kassim, S. Padmanabhan, J. McGrath, M. Pemble, Preparation and Properties of Silica Inverse Opal via Self-Assembly, Applied Mechanics and Materials, Trans Tech Publ, 2015, pp. 318–324.

[67] A.A. Zakhidov, I.I. Khayrullin, R.H. Baughman, Z. Iqbal, K. Yoshino, Y. Kawagishi, S. Tatsuhara, CVD synthesis of carbon-based metallic photonic crystals, Nanostruct. Mater. 12 (5–8) (1999) 1089–1095.

[68] Y. Xia, B. Gates, Y. Yin, Y.J.A.M. Lu, Monodispersed colloidal spheres: old materials with new applications, Adv. Mater. 12 (10) (2000) 693–713.

[69] X. Zhao, F. Su, Q. Yan, W. Guo, X.Y. Bao, L. Lv, Z. Zhou, Templating methods for preparation of porous structures, J. Mater. Chem. 16 (7) (2006) 637–648.

[70] A. Morelos-Gómez, P.G. Mani-González, A.E. Aliev, E. Muñoz-Sandoval, A. Herrera-Gómez, A.A. Zakhidov, H. Terrones, M. Endo, M. Terrones, Controlling the optical, electrical and chemical properties of carbon inverse opal by nitrogen doping, Adv. Funct. Mater. 24 (18) (2014) 2612–2619.

[71] D.-Y. Kang, S.-O. Kim, Y.J. Chae, J.K. Lee, J.H. Moon, Particulate inverse opal carbon electrodes for lithium-ion batteries, Langmuir 29 (4) (2013) 1192–1198.

[72] N. Tachikawa, K. Yamauchi, E. Takashima, J.-W. Park, K. Dokko, M. Watanabe, Reversibility of electrochemical reactions of sulfur supported on inverse opal carbon in glyme–Li salt molten complex electrolytes, Chem. Commun. 47 (28) (2011) 8157–8159.

[73] S. Tabata, Y. Isshiki, M. Watanabe, Inverse opal carbons derived from a polymer precursor as electrode materials for electric double-layer capacitors, J. Electrochem. Soc. 155 (3) (2008) K42–K49.

[74] X. Song, R. Kanzaki, S.-i. Ishiguro, Y.J.A.S. Umebayashi, Physicochemical and acid-base properties of a series of 2-Hydroxyethylammonium-based protic ionic liquids, Anal. Sci. 28 (5) (2012) 469–474.

[75] H. Fudouzi, Y.J.A.M. Xia, Photonic papers and inks: color writing with colorless materials, Adv. Mater. 15 (11) (2003) 892–896.

[76] S.H. Foulger, P. Jiang, A.C. Lattam, D.W. Smith, J.J.L. Ballato, Mechanochromic response of poly (ethylene glycol) methacrylate hydrogel encapsulated crystalline colloidal arrays, Langmuir 17 (19) (2001) 6023–6026.

[77] R.A. Barry, P.J.L. Wiltzius, Humidity-sensing inverse opal hydrogels, Langmuir 22 (3) (2006) 1369–1374.

[78] J. Shin, P.V. Braun, W. Lee, Fast response photonic crystal pH sensor based on templated photo-polymerized hydrogel inverse opal, Sensor. Actuator. B Chem. 150 (1) (2010) 183–190.

[79] H. Zhao, J. Gao, Z. Pan, G. Huang, X. Xu, Y. Song, R. Xue, W. Hong, H. Qiu, Chemically responsive polymer inverse-opal photonic crystal films created by a self-assembly method, J. Phys. Chem. 120 (22) (2016) 11938–11946.

[80] Y. Zhu, H. Cao, L. Tang, X. Yang, C. Li, Immobilization of horseradish peroxidase in three-dimensional macroporous TiO2 matrices for biosensor applications, Electrochim. Acta 54 (10) (2009) 2823–2827.

[81] W. Shen, M. Li, B. Wang, J. Liu, Z. Li, L. Jiang, Y. Song, Hierarchical optical antenna: gold nanoparticle-modified photonic crystal for highly-sensitive label-free DNA detection, J. Mater. Chem. 22 (16) (2012) 8127–8133.

[82] J. Li, X. Zhao, H. Wei, Z.-Z. Gu, Z. Lu, Macroporous ordered titanium dioxide (TiO2) inverse opal as a new label-free immunosensor, Anal. Chim. Acta 625 (1) (2008) 63–69.

[83] W. Qian, Z.-Z. Gu, A. Fujishima, O. Sato, Three-dimensionally ordered macroporous polymer materials: an approach for biosensor applications, Langmuir 18 (11) (2002) 4526–4529.

[84] D.J. Monk, D.R.J.A. Walt, Optical fiber-based biosensors, Anal. Bioanal. Chem. 379 (7–8) (2004) 931–945.

[85] R.C. Schroden, M. Al-Daous, C.F. Blanford, A.J.C.o.m. Stein, Optical properties of inverse opal photonic crystals, Chem. Mater. 14 (8) (2002) 3305–3315.

[86] L. Xia, J. Song, R. Xu, D. Liu, B. Dong, L. Xu, H.J.B. Song, Zinc oxide inverse opal electrodes modified by glucose oxidase for electrochemical and photoelectrochemical biosensor, Biosens. Bioelectron. 59 (2014) 350–357.

[87] X. Zhao, J. Xue, Z. Mu, Y. Huang, M. Lu, Z. Gu, Gold nanoparticle incorporated inverse opal photonic crystal capillaries for optofluidic surface enhanced Raman spectroscopy, Biosens. Bioelectron. 72 (2015) 268–274.

[88] E. Chow, A. Grot, L. Mirkarimi, M. Sigalas, G. Girolami, Ultracompact biochemical sensor built with two-dimensional photonic crystal microcavity, Opt. Lett. 29 (10) (2004) 1093–1095.

[89] A. Baryshev, R. Fujikawa, A. Khanikaev, A. Granovsky, K.-H. Shin, P.-B. Lim, M. Inoue, Mesoporous Photonic Crystals for Sensor Applications, Photonic Crystals and Photonic Crystal Fibers for Sensing Applications II, International Society for Optics and Photonics, 2006, p. 63690B.

[90] F. Fathi, M.R. Rashidi, Y. Omidi, Ultra-sensitive Detection by Metal Nanoparticles-Mediated Enhanced SPR Biosensors, Talanta, 192, Talanta, 2018, pp. 118–127.

[91] F. Fathi, R. Rahbarghazi, A.A. Movassaghpour, M.-R. Rashidi, Detection of CD133-marked cancer stem cells by surface plasmon resonance: its application in leukemia patients, Biochim Biophys Acta (BBA)-General Subjects, 2019.

[92] T. Schricker, H. Sato, T. Beaudry, T. Codere, R. Hatzakorzian, J.C. Pruessner, Intraoperative maintenance of normoglycemia with insulin and glucose preserves verbal learning after cardiac surgery, PloS One 9 (6) (2014), e99661.

[93] R. Monošík, M. Streďanský, K. Lušpai, P. Magdolen, E.J.E. Šturdík, m. technology, Amperometric glucose biosensor utilizing FAD-dependent glucose dehydrogenase immobilized on nanocomposite electrode, Enzym. Microb. Technol. 50 (4–5) (2012) 227–232.

[94] E.H. Yoo, S.Y. Lee, Glucose biosensors: an overview of use in clinical practice, Sensors (Basel, Switzerland) 10 (5) (2010) 4558–4576.

[95] S. Yusan, M.M. Rahman, N. Mohamad, T.M. Arrif, A.Z.A. Latif, M.A. Ma, W.S. B. Wan Nik, Development of an amperometric glucose biosensor based on the immobilization of glucose oxidase on the Se-MCM-41 mesoporous composite, J. Anal. Methods Chem. (2018) 2018.

[96] C.M. Miyazaki, F.M. Shimizu, J. Mejía-Salazar, O.N. Oliveira Jr., M. Ferreira, Surface plasmon resonance biosensor for enzymatic detection of small analytes, Nanotechnology 28 (14) (2017) 145501.

[97] L. Kumar, R. Gupta, D. Thakar, V. Vibhu, S. Annapoorni, A new route to glucose sensing based on surface plasmon resonance using polyindole, Plasmonics 8 (2) (2013) 487–494.

[98] D. Tang, Q. Li, J. Tang, B. Su, G. Chen, An enzyme-free quartz crystal microbalance biosensor for sensitive glucose detection in biological fluids based on glucose/dextran displacement approach, Anal. Chim. Acta 686 (1–2) (2011) 144–149.

[99] J. Kim, C. Son, S. Choi, W.J. Yoon, H. Ju, A plasmonic fiber based glucometer and its temperature dependence, Micromachines 9 (10) (2018) 506.

[100] Q. Gao, Y. Guo, W. Zhang, H. Qi, C. Zhang, An amperometric glucose biosensor based on layer-by-layer GOx-SWCNT conjugate/redox polymer multilayer on a screen-printed carbon electrode, Sensor. Actuator. B Chem. 153 (1) (2011) 219–225.

[101] X. You, J.H. Pikul, W.P. King, J.J. Pak, Zinc oxide inverse opal enzymatic biosensor, Appl. Phys. Lett. 102 (25) (2013) 253103.

[102] L. Jin, Y. Zhao, X. Liu, Y. Wang, B. Ye, Z. Xie, Z. Gu, Dual signal glucose reporter based on inverse opal conducting hydrogel films, Soft Matter 8 (18) (2012) 4911–4917.

[103] S. Nadzirah, U. Hashim, M. Rusop, Development of DNA biosensor based on TiO2 nanoparticles. AIP Conference Proceedings, AIP Publishing, 2018, 020062.

[104] C. Hu, X. Zhang, W. Li, Y. Yan, G. Xi, H. Yang, J. Li, H. Bai, Large-scale, ultrathin and (001) facet exposed TiO 2 nanosheet superstructures and their applications in photocatalysis, J. Mater. Chem. A 2 (7) (2014) 2040–2043.

[105] T. Mavrič, M. Benčina, R. Imani, I. Junkar, M. Valant, V. Kralj-Iglič, A. Iglič, Electrochemical biosensor based on TiO2 nanomaterials for cancer diagnostics, Advances in Biomembranes and Lipid Self-Assembly, Elsevier2018, pp. 63-105.

[106] H.A.R.A. Hussian, M.A.M. Hassan, I.R. Agool, Synthesis of titanium dioxide (TiO2) nanofiber and nanotube using different chemical method, Optik-Int. J. Light Elect. Opt. 127 (5) (2016) 2996–2999.

[107] H. Cao, Y. Zhu, L. Tang, X. Yang, C. Li, A glucose biosensor based on immobilization of glucose oxidase into 3D macroporous TiO2, Electroanalysis: Int. J. Dev. Fundament. Pract. Aspects Electroanal. 20 (20) (2008) 2223–2228.

[108] X. Feng, J. Xu, Y. Liu, W. Zhao, Visual sensors of an inverse opal hydrogel for the colorimetric detection of glucose, J. Mater. Chem. B. 7 (22) (2019) 3576–3581.

[109] Y.-J. Lee, S.A. Pruzinsky, P.V.J.L. Braun, Glucose-sensitive inverse opal hydrogels: analysis of optical diffraction response, Langmuir 20 (8) (2004) 3096–3106.

[110] M. Honda, K. Kataoka, T. Seki, Y.J.L. Takeoka, Confined stimuli-responsive polymer gel in inverse opal polymer membrane for colorimetric glucose sensor, Langmuir 25 (14) (2009) 8349–8356.

[111] E. Choi, Y. Choi, Y.H.P. Nejad, K. Shin, J. Park, Label-free specific detection of immunoglobulin G antibody using nanoporous hydrogel photonic crystals, Sensor. Actuator. B Chem. 180 (2013) 107–113.

[112] X. Feng, J. Xu, Y. Liu, W. Zhao, Visual sensors of an inverse opal hydrogel for the colorimetric detection of glucose, J. Mater. Chem. B 7 (22) (2019) 3576–3581.

[113] M. Dabrowski, M. Cieplak, P.S. Sharma, P. Borowicz, K. Noworyta, W. Lisowski, F. d'Souza, A. Kuhn, W. Kutner, Hierarchical templating in deposition of semi-covalently imprinted inverse opal polythiophene film for femtomolar determination of human serum albumin, Biosens. Bioelectron. 94 (2017) 155–161.

[114] Z. Mu, X. Zhao, Y. Huang, M. Lu, Z.J.S. Gu, Photonic crystal hydrogel enhanced plasmonic staining for multiplexed protein analysis, Small 11 (45) (2015) 6036–6043.

[115] R. Xu, Y. Jiang, L. Xia, T. Zhang, L. Xu, S. Zhang, D. Liu, H. Song, A sensitive photoelectrochemical biosensor for AFP detection based on ZnO inverse opal

electrodes with signal amplification of CdS-QDs, Biosens. Bioelectron. 74 (2015) 411–417.
[116] Y. Jiang, D. Liu, Y. Yang, R. Xu, T. Zhang, K. Sheng, H.J.S.r. Song, Photoelectrochemical detection of alpha-fetoprotein based on ZnO inverse opals structure electrodes modified by Ag 2 S nanoparticles, Sci. Rep. 6 (2016) 38400.
[117] E. Choi, Y. Choi, Y.H.P. Nejad, K. Shin, J.J.S. Park Ab, Chemical, Label-free specific detection of immunoglobulin G antibody using nanoporous hydrogel photonic crystals 180 (2013) 107–113.
[118] D.I. Fried, F.J. Brieler, M.J.C. Froeba, Designing inorganic porous materials for enzyme adsorption and applications in biocatalysis, ChemCatChem 5 (4) (2013) 862–884.
[119] Q. Zhao, J. Sun, H. Ren, Q. Zhou, Q. Lin, Horseradish peroxidase immobilized in macroporous hydrogel for acrylamide polymerization, J. Polym. Sci. Polym. Chem. 46 (6) (2008) 2222–2232.
[120] G.Y. Tonga, Y. Jeong, B. Duncan, T. Mizuhara, R. Mout, R. Das, S.T. Kim, Y.-C. Yeh, B. Yan, S.J.N.c. Hou, Supramolecular regulation of bioorthogonal catalysis in cells using nanoparticle-embedded transition metal catalysts, Nat. Chem. 7 (7) (2015) 597.
[121] M. Riedel, F.J.A.a.m. Lisdat, Integration of enzymes in polyaniline-sensitized 3D inverse opal TiO2 architectures for light-driven biocatalysis and light-to-current conversion, ACS Appl. Mater. Interfaces 10 (1) (2018) 267–277.
[122] Y. Jiang, C. Cui, Y. Huang, X. Zhang, J.J.C.C. Gao, Enzyme-based inverse opals: a facile and promising platform for fabrication of biocatalysts, Chem. Commun. 50 (41) (2014) 5490–5493.
[123] M.G. Torres, M. Foresti, M.J.B.e.j. Ferreira, Effect of different parameters on the hydrolytic activity of cross-linked enzyme aggregates (CLEAs) of lipase from Thermomyces lanuginosa, Biochem. Eng. J. 72 (2013) 18–23.
[124] Y. Jiang, C. Cui, Y. Huang, X. Zhang, J. Gao, Enzyme-based inverse opals: a facile and promising platform for fabrication of biocatalysts, Chem. Commun. 50 (41) (2014) 5490–5493.
[125] H. Wang, H. Gu, Z. Chen, L. Shang, Z. Zhao, Z. Gu, Y.J.A.a.m. Zhao, Enzymatic inverse opal hydrogel particles for biocatalyst, ACS Appl. Mater. Interfaces 9 (15) (2017) 12914–12918.
[126] E.J.C.S.R. Magner, Immobilisation of enzymes on mesoporous silicate materials, Chem. Soc. Rev. 42 (15) (2013) 6213–6222.
[127] W. Lee, T. Kang, S.-H. Kim, J. Jeong, An antibody-immobilized silica inverse opal nanostructure for label-free optical biosensors, Sensors 18 (1) (2018) 307.
[128] B. Maeng, Y. Park, J. Park, Direct label-free detection of Rotavirus using a hydrogel based nanoporous photonic crystal, RSC Adv. 6 (9) (2016) 7384–7390.
[129] A. Chiappini, L. Pasquardini, S. Nodehi, C. Armellini, N. Bazzanella, L. Lunelli, S. Pelli, M. Ferrari, S. Pietralunga, Fluorescent aptamer immobilization on inverse colloidal crystals, Sensors 18 (12) (2018) 4326.
[130] W. Shen, M. Li, B. Wang, J. Liu, Z. Li, L. Jiang, Y. Song, Hierarchical optical antenna: gold nanoparticle-modified photonic crystal for highly-sensitive label-free DNA detection, J. Mater. Chem. 22 (16) (2012) 8127–8133.
[131] Y. Zhao, X. Zhao, B. Tang, W. Xu, J. Li, J. Hu, Z. Gu, Quantum-dot-tagged bioresponsive hydrogel suspension array for multiplex label-free DNA detection, Adv. Funct. Mater. 20 (6) (2010) 976–982.
[132] L. He, J. Huang, T. Xu, L. Chen, K. Zhang, S. Han, Y. He, S.T. Lee, Silver nanosheet-coated inverse opal film as a highly active and uniform SERS substrate, J. Mater. Chem. 22 (4) (2012) 1370–1374.
[133] T. Cassagneau, F. Caruso, Inverse opals for optical affinity biosensing, Adv. Mater. 14 (22) (2002) 1629–1633.
[134] S. Liu, A. Chen, Coadsorption of horseradish peroxidase with thionine on TiO2 nanotubes for biosensing, Langmuir 21 (18) (2005) 8409–8413.
[135] A.L. Clem, J. Sims, S. Telang, J.W. Eaton, J. Chesney, Virus detection and identification using random multiplex (RT)-PCR with 3'-locked random primers, Virol. J. 4 (1) (2007) 65.
[136] M.F. Pineda, L.L.-Y. Chan, T. Kuhlenschmidt, C.J. Choi, M. Kuhlenschmidt, B. T. Cunningham, Rapid specific and label-free detection of porcine rotavirus using photonic crystal biosensors, IEEE Sensor. J. 9 (4) (2009) 470–477.
[137] T. Endo, S. Ozawa, N. Okuda, Y. Yanagida, S. Tanaka, T. Hatsuzawa, Reflectometric detection of influenza virus in human saliva using nanoimprint lithography-based flexible two-dimensional photonic crystal biosensor, Sensor. Actuator. B Chem. 148 (1) (2010) 269–276.
[138] Z. Nie, E. Kumacheva, Patterning surfaces with functional polymers, Nat. Mater. 7 (4) (2008) 277.
[139] L.F. Pease III, P. Deshpande, Y. Wang, W.B. Russel, S.Y. Chou, Self-formation of sub-60-nm half-pitch gratings with large areas through fracturing, Nat. Nanotechnol. 2 (9) (2007) 545.
[140] B. Hatton, L. Mishchenko, S. Davis, K.H. Sandhage, J. Aizenberg, Assembly of large-area, highly ordered, crack-free inverse opal films, Proc. Natl. Acad. Sci. Unit. States Am. 107 (23) (2010) 10354–10359.
[141] B.T. Cunningham, P. Li, S. Schulz, B. Lin, C. Baird, J. Gerstenmaier, C. Genick, F. Wang, E. Fine, L. Laing, Label-free assays on the BIND system, J. Biomol. Screen 9 (6) (2004) 481–490.
[142] H. Su, X.R. Cheng, T. Endo, K. Kerman, Photonic crystals on copolymer film for label-free detection of DNA hybridization, Biosens. Bioelectron. 103 (2018) 158–162.
[143] M. Li, F. He, Q. Liao, J. Liu, L. Xu, L. Jiang, Y. Song, S. Wang, D. Zhu, Ultrasensitive DNA detection using photonic crystals, Angew. Chem. 120 (38) (2008) 7368–7372.
[145] S. Gao, N. Koshizaki, H. Tokuhisa, E. Koyama, T. Sasaki, J.K. Kim, J. Ryu, D. S. Kim, Y.J.A.F.M. Shimizu, Highly stable Au nanoparticles with tunable spacing and their potential application in surface plasmon resonance biosensors, Adv. Funct. Mater. 20 (1) (2010) 78–86.
[146] Y. An, X. Jiang, W. Bi, H. Chen, L. Jin, S. Zhang, C. Wang, W. Zhang, Sensitive electrochemical immunosensor for α-synuclein based on dual signal amplification using PAMAM dendrimer-encapsulated Au and enhanced gold nanoparticle labels, Biosens. Bioelectron. 32 (1) (2012) 224–230.
[147] P. Xu, N.H. Mack, S.-H. Jeon, S.K. Doorn, X. Han, H.-L.J.L. Wang, Facile fabrication of homogeneous 3D silver nanostructures on gold-supported polyaniline membranes as promising SERS substrates, Langmuir 26 (11) (2010) 8882–8886.
[148] G. Liu, W. Cai, L. Kong, G. Duan, F. Lü, Vertically cross-linking silver nanoplate arrays with controllable density based on seed-assisted electrochemical growth and their structurally enhanced SERS activity, J. Mater. Chem. 20 (4) (2010) 767–772.
[149] L. He, J. Huang, T. Xu, L. Chen, K. Zhang, S. Han, Y. He, S.T. Lee, Silver nanosheet-coated inverse opal film as a highly active and uniform SERS substrate, J. Mater. Chem. 22 (4) (2012) 1370–1374.
[150] K. Vindas, L. Leroy, P. Garrigue, S. Voci, T. Livache, S. Arbault, N. Sojic, A. Buhot, E. Engel, Highly parallel remote SPR detection of DNA hybridization by micropillar optical arrays, Anal. Bioanal. Chem. 411 (11) (2019) 2249–2259.
[151] D. Kawasaki, H. Yamada, K. Maeno, K. Sueyoshi, H. Hisamoto, T. Endo, Core–shell-structured gold nanocone array for label-free DNA sensing, ACS Appl. Nano Mater. 2 (8) (2019) 4983–4990.
[152] B. Amini, M. Kamali, M. Salouti, P. Yaghmaei, Spectrophotometric, colorimetric and visually detection of Pseudomonas aeruginosa ETA gene based gold nanoparticles DNA probe and endonuclease enzyme, Spectrochim. Acta A 199 (2018) 421–429.
[153] A. Heim, C. Ebnet, G. Harste, P. Pring-Åkerblom, Rapid and quantitative detection of human adenovirus DNA by real-time PCR, Journal of medical virology, J. Med. Virol. 70 (2) (2003) 228–239.
[154] Q. Li, S. Zhou, T. Zhang, B. Zheng, H. Tang, Bioinspired sensor chip for detection of miRNA-21 based on photonic crystals assisted cyclic enzymatic amplification method, Biosens. Bioelectron. 150 (2020) 111866.
[155] L. Gervais, N. De Rooij, E. Delamarche, Microfluidic chips for point-of-care immunodiagnostics, Adv. Mater. 23 (24) (2011) H151–H176.
[156] Y. Xu, H. Wang, C. Luan, Y. Liu, B. Chen, Y.J.B. Zhao, Bioelectronics, aptamer-based hydrogel barcodes for the capture and detection of multiple types of pathogenic bacteria, Biosens. Bioelectron vol. 100 (2018) 404–410.
[157] X. Zhao, J. Xue, Z. Mu, Y. Huang, M. Lu, Z.J.B. Gu, Gold nanoparticle incorporated inverse opal photonic crystal capillaries for optofluidic surface enhanced Raman spectroscopy, Biosens. Bioelectron. 72 (2015) 268–274.
[158] Q. Zhong, Z. Xie, H. Ding, C. Zhu, Z. Yang, Z. Gu, Carbon inverse opal rods for nonenzymatic cholesterol detection, Small 11 (43) (2015) 5766–5770.
[159] Y. Xu, H. Wang, C. Luan, Y. Liu, B. Chen, Y. Zhao, Aptamer-based hydrogel barcodes for the capture and detection of multiple types of pathogenic bacteria, Biosens. Bioelectron. 100 (2018) 404–410.
[160] W.-K. Kuo, H.-P. Weng, J.-J. Hsu, H. Yu, Photonic crystal-based sensors for detecting alcohol concentration, Appl. Sci. 6 (3) (2016) 67.
[161] S.K. Srivastava, R. Verma, B.D. Gupta, Surface plasmon resonance based fiber optic sensor for the detection of low water content in ethanol, Sensor. Actuator. B Chem. 153 (1) (2011) 194–198.
[162] X. Hu, G. Li, M. Li, J. Huang, Y. Li, Y. Gao, Y. Zhang, Ultrasensitive specific stimulant assay based on molecularly imprinted photonic hydrogels, Adv. Funct. Mater. 18 (4) (2008) 575–583.
[163] W.P. Hall, S.N. Ngatia, R.P.J.T. Van Duyne, LSPR biosensor signal enhancement using nanoparticle– antibody conjugates, J. Phys. Chem. C 115 (5) (2011) 1410–1414.
[164] F. Fathi, A. Rezabakhsh, R. Rahbarghazi, M.-R.J.B. Rashidi, Bioelectronics, Early-stage detection of VE-cadherin during endothelial differentiation of human mesenchymal stem cells using SPR biosensor, Biosens. Bioelectron. 96 (2017) 358–366.
[165] L. Wang, R. Yan, Z. Huo, L. Wang, J. Zeng, J. Bao, X. Wang, Q. Peng, Y. Li, Fluorescence resonant energy transfer biosensor based on upconversion-luminescent nanoparticles, Angew. Chem., Int. Ed. Engl. 44 (37) (2005) 6054–6057.
[166] M. Mansouri, F. Fathi, R. Jalili, S. Shoeibie, S. Dastmalchi, A. Khataee, M.-R. Rashidi, SPR enhanced DNA biosensor for sensitive detection of donkey meat adulteration, Food Chem. (2020) 127163.
[167] S.M. Shamah, B.T.J.A. Cunningham, Label-free cell-based assays using photonic crystal optical biosensors, Analyst 136 (6) (2011) 1090–1102.
[168] X. You, J.H. Pikul, W.P. King, J. Pak, Zinc oxide inverse opal enzymatic biosensor, Appl. Phys. Lett. 102 (25) (2013) 253103.
[169] L. Wang, Q. Yan, X.J.L. Zhao, From planar defect in opal to planar defect in inverse opal, Langmuir 22 (8) (2006) 3481–3484.
[170] S. Hosseini, P. Vázquez-Villegas, M. Rito-Palomares, S.O. Martinez-Chapa, Advantages, disadvantages and modifications of conventional ELISA, enzyme-linked immunosorbent assay (ELISA), Springer2018, pp. 67-115.